Optimizing protein S-acylation detection in autophagy

by

Meng Qi Liao

A thesis
presented to the University of Waterloo
in fulfillment of the
thesis requirement for the degree of
Master of Science
in
Biology

Waterloo, Ontario, Canada, 2021

Author's Declaration

I hereby declare that I am the sole author of this thesis. This is a true copy of the thesis, including any required final revisions, as accepted by my examiners.

I understand that my thesis may be made electronically available to the public.

Abstract

S-acylation, sometimes referred to as S-palmitoylation or simply palmitoylation, is a posttranslational protein modification involving the covalent addition of a fatty acid to cysteine residues. Since the first characterization of protein palmitoylation over 40 years ago, this modification has been implicated in a variety of cellular processes, particularly membrane targeting, protein localization, and regulation of protein-protein interactions. These processes are essential in autophagy, a membrane-dependent cellular recycling and degradation mechanism to remove damaged organelles and toxic proteins. Due to its unique reversibility among lipid modifications as well its regulatory roles in membrane-dependent processes essential to autophagy, palmitoylation has recently began to be explored in the context of autophagy. Despite increasing evidence pointing to a regulatory role of palmitoylation in autophagy, methods for the detection of palmitoylated proteins specifically under autophagic conditions have not been a focus for development and optimization. The aim of this thesis project was to optimize detection methods of palmitoylated proteins during autophagy. In this regard, we combined existing techniques of chemical autophagy induction, metabolic labeling with bio-orthogonal fatty acid analogs that are detectable with click chemistry, as well as affinity purification for the detection and identification of palmitoylated proteins during autophagy. First, we tested several new commercial products and established a working protocol for the click chemistry assay. We then demonstrated that delivery of detectable alkynyl fatty acids into cells during metabolic labeling can be considerably improved with the use of delipidated media and saponification of fatty acids. Cellular incorporation of the 18-carbon alkynyl stearate, the most commonly used fatty acid analog, was shown to be improved the most through saponification and incubation with fatty acid free bovine serum albumin (BSA), leading to greater availability of the fatty acid label and significantly enhanced overall palmitoylation signal. In addition, saponification of fatty acids prior to addition to

cell culture can protect cells from lipotoxicity and activation of stress pathways induced by the direct addition of fatty acids. Next, we tested two approaches to enrich and purify palmitoylated proteins following click chemistry linkage of an affinity probe. In addition, we determined optimal treatment times of autophagy induction using rapamycin to induce the most robust autophagic flux. Finally, we demonstrated low throughput confirmation and characterization of palmitoylation in two proteins of interest, the small VCP-interacting protein and the spike protein of the SARS-CoV2 virus, via immunoprecipitation and click chemistry detection. The established methods and findings of this study provide important foundations to identify palmitoylation targets and characterize pathways of palmitoylation regulation during autophagy, which ultimately will provide valuable insight on the molecular mechanisms of a wide range of diseases from cancer to neurodegeneration.

Acknowledgements

First and foremost, I would like to thank my supervisor, Dr. Dale Martin for everything. Thank you for seeing my passion for biology and giving me the chance to be a part of your lab. You taught me how to be a researcher, how to be a graduate student, and what it means to be a great teacher. Your continuing support, patience and faith in me are the reasons for all I have accomplished, especially through this incredibly difficult time in the midst of a pandemic.

I would also like to thank past and present members of the NeurdyPhagy (Martin) lab, Dr. Firyal Ramzan, Dr. Muneera Fayaad, Gyan and our undergraduate students Fatima, Arshpreet, and Yasaman for all of your work and for making the lab a wonderful place to be. Thank you especially Firyal for your support and companionship on the other side of the bench and beyond, for listening and giving advice when I felt overwhelmed, and for offering help whenever I needed it. It is truly a pleasure to work among all of you.

I would like to thank the Department of Biology and the donors for the Ram and Lekha Tumkur Memorial Bursary, as well as IODE Ontario for the Lucy Morrison Memorial Award in support of my graduate work. In addition, I would like to thank Dr. Gareth Thomas for providing the zDHHC vectors, Dr. Michael Beazely for providing the HT22 cells, Dr. Luc Bertiaume for the gift of the ctHTT-GFP constructs, and Dr. Martin and Dr. Firyal Ramzan for performing the necessary cloning.

Last but not least, I would like to thank my family for their love and support since I have become a part of it. And to Michael, my rock and my other half through thick and thin, for better or worse, thank you for making me laugh even in the most impossible moments, thank you for giving me the strength to get through anything and making me believe that I can achieve everything. I would never have become the person I am today without you.

Table of Contents

List of Figures

List of Tables

List of Abbreviations

2BP	2-bromopalmitate
ABE	Acyl-biotin exchange
Acyl-RAC	Acyl resin-assisted capture
AMPK	AMP-activated protein kinase
APT	Acyl protein thioesterase
ATG	Autophagy-related gene
βme	B-mercaptoethanol
Co-IP	Co-immunoprecipitation
DCC-FBS	Dextran charcoal coated fetal bovine serum
DMSO	Dimethyl sulfoxide
DTT	Dithiothreitol
EDTA	Ethylenediaminetetraacetic acid
FAFBSA	Fatty acid-free bovine serum albumin
HAM	Hydroxylamine
HEPES	4-(2-hydroxyethyl)-1-piperazineethanesulfonic acid
IF	Immunofluorescence
IP	Immunoprecipitation
LC3 (MAPI-LC3)	Microtubule-associated proteins 1A/1B light chain 3
MOPS	3-(N-morpholino) propanesulfonic acid
MS	Mass spectrometry
mTOR	Mammalian target of rapamycin
NEM	N-ethylmaleimide
PAT	Protein S-acyltransferase
PE	Phosphatidylethanolamine
PVDF	Polyvinylidene fluoride
SDS	Sodium dodecyl sulfate
SILAC	Stable isotope labeling by amino acids in cell culture
SLB	Sample loading buffer
SQSTM1	Sequestosome 1
SVIP	Small valosin-containing protein/p97-interacting protein
TBTA	Tris-(benzyltriazolylmethyl) amine
TCEP-HCl	Tris-carboxyethylphosphine hydrochloride
VCP	Valosin-containing protein

Chapter 1

Introduction

Protein posttranslational modifications govern many aspects of protein function. Fatty acylation involves the covalent addition of short and long-chain fatty acids to proteins (Zaballa & van der Goot, 2018). In particular, S-acylation serves to regulate a myriad of cellular processes, especially those involved in protein trafficking and membrane interactions. For these reasons, the Martin lab is interested in the role of S-acylation in autophagy, a lysosomal clearance and degradation mechanism that is heavily dependent on these processes (Parzych & Klionsky, 2013). Since autophagy is often impaired in neurodegenerative diseases leading to a buildup of toxic protein aggregates, therefore, gaining insights on how autophagy may be regulated by S-acylation may identify novel therapeutic targets. The present thesis aimed to optimize detection of protein S-acylation during cellular autophagy. Through these experiments, we aimed to amplify the sensitivity of detection of such proteins to enable further characterizations of how they are S-acylated, as well as how this modification contributes to their functioning.

1.1 Protein S-acylation

Fatty acylation predominantly refers to S-acylation and N-myristoylation. The term S-acylation is used interchangeably with S-palmitoylation, or simply palmitoylation, owing to the 16-carbon palmitic acid being the most common fatty acid in cells, and therefore probably the most preferred (Linder & Deschenes, 2007; Zaballa & van der Goot, 2018). S-acylation occurs between the thiol group on the cysteine residue of the target protein and the carbonyl carbon of the fatty acid (Figure 1.1A), resulting in a labile thioester bond which can be dynamically regulated by enzymes (Sanders et al., 2015; Zaballa & van der Goot, 2018). On the other hand, N-myristoylation refers to the addition of the 14-carbon myristic acid to N-terminal glycines, and sometimes lysines, through an amide bond

(Resh, 2016; Stevenson et al., 1992). Since the first discovery and characterization of protein S-acylation in the 70's (Braun & Radin, 1969; Schmidt et al., 1979), over 5000 proteins have been identified as substrates by the time of the creation of SwissPalm in 2015, an online database of palmitoylated proteins (Blanc et al., 2015). Frequency analysis of another systems-wide curation of palmitoylated proteins, Swiss-prot, estimated more than 10% of the proteome to be palmitoylated (Khoury et al., 2011). Therefore, it is reasonable to conclude that protein palmitoylation plays an important role in numerous cellular processes.

Protein palmitoylation is highly conserved among eukaryotes (Zaballa & van der Goot, 2018). The importance of palmitoylation regulation of protein functions has been underestimated due to the technical difficulties in detection. However, with recent advances in new efficient, rapid, and sensitive detection methods, palmitoylation has begun to emerge as an important mechanism. The unique reversibility of S-acylation among all lipid modifications makes it an interesting candidate for regulatory roles by enabling rapid and dynamic signaling, similar to phosphorylation (Sanders et al., 2015). A study in 2015 by Sanders, Martin and colleagues compiled all mammalian palmitoylproteome studies to date and performed enrichment analysis on cellular functions of palmitoylated proteins. The study revealed a high percentage of palmitoylation enriched in neuronal processes including synaptic vesicle fusion and recycling, which supported the importance of palmitoylation in the brain and neurodegenerative disorders (Sanders et al., 2015).

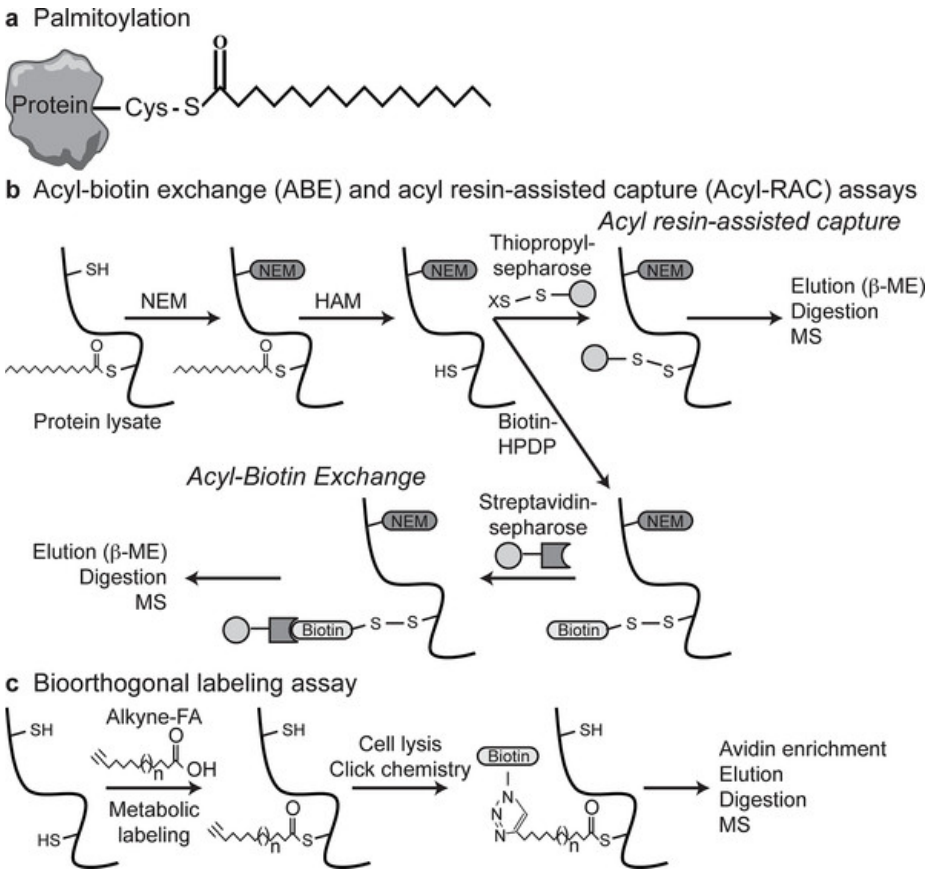

Figure 1.1 Protein palmitoylation and detection methods.

(A) Palmitoylation involves the reversible addition of long-chain fatty acids (FA) to cysteine residues via thioester bonds. (B) The ABE and Acyl-RAC assays use N-ethylmaleimide (NEM) to block free cysteines and hydroxylamine (HAM) to remove palmitate. The Acyl-RAC assay uses thiopropyl-sepharose beads that covalently react with the free cysteines, allowing enrichment and elution, using β-mercaptoethanol (βME), of palmitoyl-proteins and detection by MS. Following HAM treatment in the ABE assay free cysteines are labeled using Biotin-HPDP, allowing streptavidin-sepharose enrichment for MS. (C) The bioorthogonal-labeling assay uses alkyne-FA analogues followed by click chemistry to covalently link alkynyl-palmitate with biotin, allowing enrichment of palmitoyl-proteins for MS (Sanders et al., 2015).

1.1.1 Mechanisms of palmitoylation and protein S-acyltransferases (PATs)

Protein palmitoylation is facilitated by a family of enzymes with the highly conserved zinc finger zDHHC (Asp-His-His-Cys) domains (Resh, 2016), referred to as protein S-acyltransferases (PATs) (Lemonidis et al., 2017; Zaballa & van der Goot, 2018). First discovered in yeast, the identification of

the zDHHC motif within a cysteine-rich domain that was required for palmitoylation led to the subsequent discovery of 23 mammalian PATs (Keller et al., 2004; Lobo et al., 2002; Roth et al., 2002).

The mammalian zDHHC enzymes typically consist of four or six transmembrane domains and the majority of the zDHHC domains are restricted to the cytosolic side (Ohno et al., 2006; Zaballa & van der Goot, 2018). Most mammalian PATs are localized to the endoplasmic reticulum (ER) and the Golgi apparatus, while a few appear at the plasma membrane (Ohno et al., 2006). A structural study of PATs by Rana and colleagues showed the transmembrane domains to have a pyramidal structure with the base containing the active site facing the cytosol, which assists in the prediction of palmitoylation substrates where proteins with cysteines close the cytosolic side of transmembrane domains are more likely to be palmitoylated (Rana et al., 2018; Reddy et al., 2016).

Protein palmitoylation occurs in two steps: first, the acyl-coenzyme A from the fatty acid forms an acyl-enzyme intermediate with the zDHHC cysteine of the PAT, then the acyl moiety is transferred from the zDHHC cysteine to the cysteine of the target protein (Figure 1.2) (Rana et al., 2018; Zaballa & van der Goot, 2018).

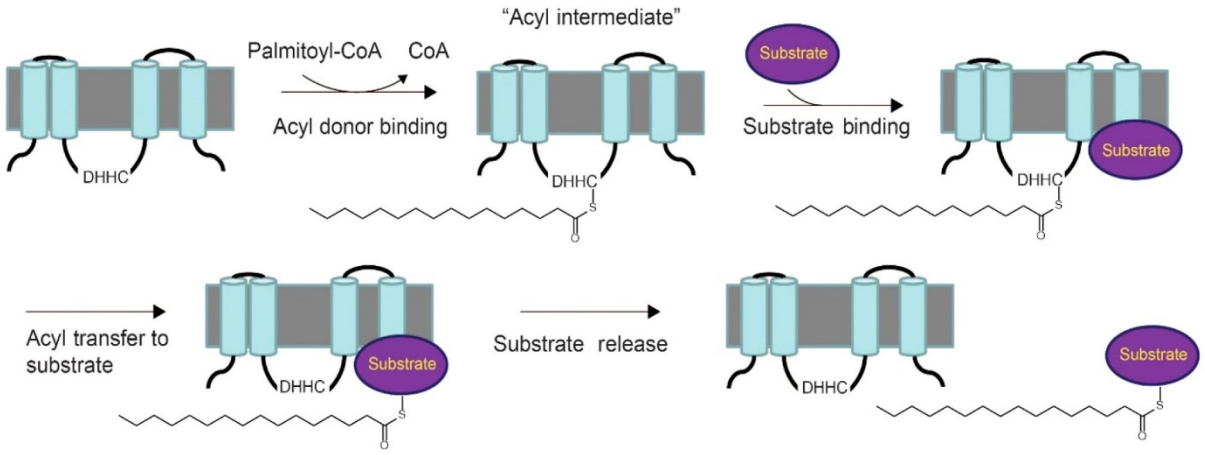

Figure 1.2 Mechanism of zDHHC-catalyzed cysteine palmitoylation.
Two-step palmitoylation mediated by protein acyltransferases (Jiang et al., 2018).

To date, no consensus sequence has been identified for palmitoylation (Jiang et al., 2018; Zaballa & van der Goot, 2018). However, there are several strategies to predict potential sites of palmitoylation. Prediction algorithms exist based on the collection of thousands of identified substrates of palmitoylation (Zhou et al., 2006). In addition, palmitoylation sites usually occur on cysteines on or near transmembrane domains or membrane-targeting domains of a protein (Jiang et al., 2018). Lastly, identification of binding motifs of protein acyltransferases may also suggest the likelihood of palmitoylation on a given protein. For example, the cytosolic N-terminal ankyrin repeat present in two of the PATs, zDHHC17 and zDHHC13, were found to recognize a consensus sequence [VIAP][VIT]XXQP on a number of known palmitoylated proteins, including huntingtin and synaptosomal-associated proteins (Lemonidis et al., 2015). Interestingly, PATs such as zDHHC17 and zDHHC13 are highly expressed in the brain, which may suggest an abundance of protein palmitoylation in the brain (Jiang et al., 2018; Lemonidis et al., 2015).

1.1.2 Enzymes of de-palmitoylation

The removal or palmitate from palmitoylated proteins, or de-palmitoylation, is mainly catalyzed by acyl protein thioesterases (APTs), which are part of the metabolic serine hydrolase superfamily (mSH) (Long & Cravatt, 2011; Won et al., 2017). Identified even before the discovery of protein acyltransferases, APT1 and APT2 in the mSH family were shown to be responsible for de-palmitoylation through a catalytic triad for the hydrolysis of the thioester bond (Won et al., 2017). In addition to APTs, the ABHD17 (alpha/beta hydrolase domain 17) family of proteins were also recently found to de-palmitoylate Ras and synaptic proteins (Lin & Conibear, 2015; Won et al., 2017). De-palmitoylation can also occur non-enzymatically through hydrolysis. The present study focuses on protein palmitoylation and its detection.

1.2 Methods of palmitoylation detection

1.2.1 Radiolabeling

The early methods of detection with the first studies of palmitoylation involved *in vitro* metabolic labeling with radioactive [^{3}H]-palmitic acid and [^{14}C]-palmitic acid, during which cells were incubated with radioactive palmitate, followed by immunoprecipitation and fluorography detection on autoradiography film (Gao & Hannoush, 2017; Zaballa & van der Goot, 2018). This method required lengthy exposure periods up to months. [^{125}I] iodo-fatty acid analogs were also available with shorter detection times but posed much higher biosafety risks requiring close health monitoring of the researchers, therefore impeded the discovery of and advancements in the studies of S-acylated proteins.

Radiolabeling was extremely slow and inefficient, therefore not suitable for combination with other proteomic techniques. This, in addition to the inability for quantitative measurement of palmitoylation, called for new detection methods. The subsequent development of both exchange and

click chemistry-based methods was many times more rapid and sensitive, thus enabling a boom in the discovery and characterization of palmitoylated proteins.

1.2.2 Bioorthogonal labeling with click chemistry

Similar to using radioactive palmitate, bioorthogonal labeling with click chemistry is also a method of metabolic labeling. However, this recent advancement poses great improvements on the radioactive metabolic labeling method. Bioorthogonal compounds were first introduced in the early 2000s and adapted for the use of metabolic labeling in palmitoylation detection (Hang et al., 2003, 2007, 2011; Heal et al., 2007; Kostiuk et al., 2008; D. D. O. Martin et al., 2008). Bioorthogonal compounds are highly selective and do not occur naturally, however, their specificity allows the study of biological processes with taggable handles (Scinto et al., 2021).

Click chemistry reaction refers to a group of chemical reactions but typically refers to the Cu(I)-catalyzed [3+2] cycloaddition which is highly specific between an alkyne and an azido group (Gao & Hannoush, 2017; Heal et al., 2008; B. R. Martin et al., 2012; Yap et al., 2010). Therefore, metabolic labeling for protein palmitoylation detection requires the use of fatty acid analogs with either an alkyne or azido handle. Cells are then incubated with the fatty acid analogs to allow cellular uptake and incorporation of the detectable fatty acids through modifications such as palmitoylation (Figure 1.1C) (Sanders et al., 2015; Zaballa & van der Goot, 2018). Proteins modified by the fatty acid analog can be detected through click chemistry linkage of a detectable probe, typically biotin or a fluorophore (Gao & Hannoush, 2017). In the case of fatty acylation, the 16-carbon alkynyl-palmitate (15-hexadecynoic acid; 15-HDYA) and 18-carbon alkynyl-stearate (17-octadecynoic acid – 17-ODYA) are used for the detection of S-palmitoylation, while the 14-carbon alkynyl-myristate (13-tetradecynoic acid; 13-TDYA) is used to detect N-myristoylation (Gao & Hannoush, 2017).

Click chemistry detection of protein palmitoylation poses several advantages. First, the nature of metabolic labeling of cells over several hours allows the capture of dynamically palmitoylated or myristoylated proteins, and therefore allows the profiling of changes in fatty acylation over a specific period of time during which treatments may be involved. Second, click chemistry detection of palmitoylated proteins is relatively rapid in comparison to exchange-based methods with fewer steps, and eliminates the acetone precipitation steps which may result in loss of protein (Liao et al., 2021). Finally, click chemistry can be combined with additional proteomic methods for downstream analysis of lipidation such as stable isotope labeling by amino acids in cell culture (SILAC), pulse-chase analysis, as well as affinity purification for mass spectrometry. There are, however, limitations to click chemistry detection. During metabolic labeling, proteins must be "available" to undergo lipidation, whereas proteins that have already been stably modified by fatty acids would be unable to take up the fatty acid analog for detection. Importantly, since metabolic labeling requires the cells to adequately incorporate the fatty acid into the cells, effective delivery is critical. The sensitivity of the assay is dependent on sufficient cellular uptake and availability of the alkynyl fatty acids within the cell, therefore inefficient delivery will inherently lead to low detection of fatty acylated proteins (Liao et al., 2021).

1.2.3 Acyl-biotin exchange (ABE) and acyl-resin assisted capture (Acyl-RAC)

In addition to metabolic labeling and click chemistry detection, cysteine-centric methods take advantage of the reversibility of the thioester bond in palmitoylation. Thioester bonds are selectively cleaved following blockage of free cysteines, leaving newly freed cysteines available for the linkage of either biotin or thiol-reactive beads in ABE or acyl-RAC, respectively (Figure 1.1B) (Sanders et al., 2015; Zaballa & van der Goot, 2018).

Exchange-based methods are considered complementary to metabolic labeling and click chemistry due to their limited detection of stably palmitoylated proteins, as well as the inability to capture palmitoylated proteins with a high turnover rate (Zaballa & van der Goot, 2018). Unfortunately, both ABE and acyl-RAC are prone to false positives due to incomplete blockage of free cysteines, cleavage of non-palmitoylation thioester bonds, and nitrosylation, which is also a cysteine modification (Majmudar & Martin, 2014; Roth et al., 2006; Zaballa & van der Goot, 2018; Zaręba-Kozioł et al., 2018).

1.3 Palmitoylation in autophagy

1.3.1 Overview of autophagy

Autophagy is one of the cells' innate waste degradation and clearance mechanisms through the lysosome. This process involves the engulfment of misfolded proteins as well as damaged organelles which are then transported to the lysosome, consequently recycling raw materials (Condello et al., 2019; Menzies et al., 2017). The term autophagy typically refers to macroautophagy, although more specific forms of autophagy exist (D. D. O. Martin et al., 2015). Under normal cellular conditions, autophagy is mainly suppressed by the mammalian target of rapamycin (mTOR)/AMP-activated protein kinase (AMPK) signaling pathway and only occurs at low basal levels to maintain homeostasis (Parzych & Klionsky, 2013; Tanida, 2011). However, autophagy is rapidly upregulated in response to several factors such as nutrient deprivation, loss of growth factors, or buildup of toxic and damaging materials (Levine & Kroemer, 2008).

The stages of autophagy involve initiation, elongation, formation of the double-membraned autophagosome, cargo loading, trafficking to lysosome, and finally fusion to lysosomes resulting in the formation of an autophagolysosome and cargo degradation (Figure 1.3) (Al-Bari, 2020; D. D. O. Martin et al., 2015). The initiation of autophagy triggers the dissociation of mTOR and prompts the

formation of an isolation membrane surrounding targets of degradation (Figure 1.3). Substrate targeting is guided by sequestosome-1 (SQSTM1), also known as p62, (Al-Bari, 2020). In order for membrane tethering and expansion of the isolation membrane to proceed, phosphatidylethanolamine (PE) must be linked to the microtubule-associated protein 1A/1B-light chain 3 (MAPI-LC3, or LC3), and the resulting LC3-II is bound to both the inner and outer membranes of the autophagosome (Parzych & Klionsky, 2013; Tanida, 2011). The mature autophagosome is then trafficked to the lysosome for fusion, resulting in the formation of the autophagolysosome which then enables degradation of the substrates along with LC3-I and p62, while LC3-II is recycled (Al-Bari, 2020; D. D. O. Martin et al., 2015; Tanida, 2011). Due to the extensive involvement of p62 and LC3, the two are often used as markers of autophagy.

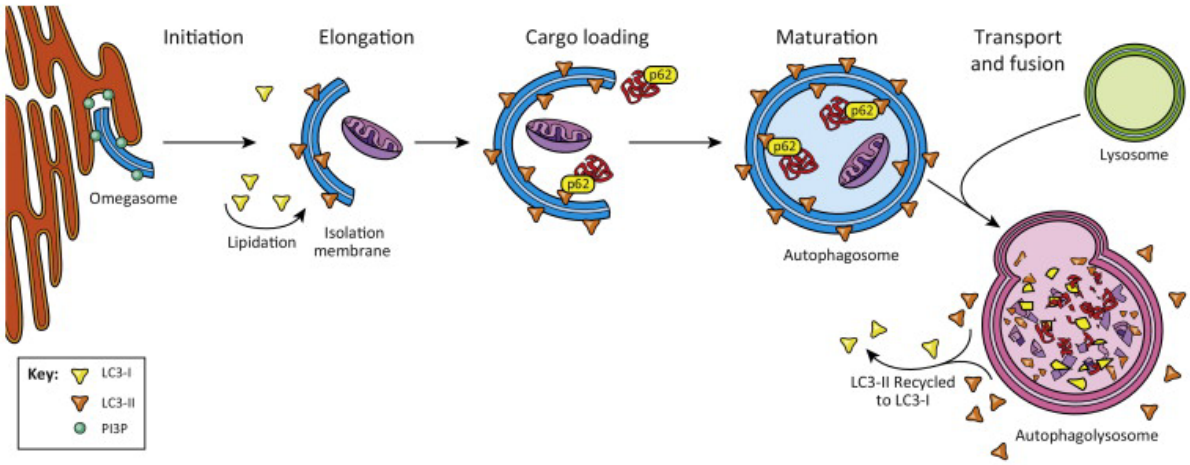

Figure 1.3 Autophagy is a membrane-dependent process.

Autophagy involves the formation of double-membraned vesicles that incorporate damaged organelles and toxic or aggregated proteins, and fuse with the lysosome for degradation (D. D. O. Martin et al., 2015).

The stages of the autophagic process can be disrupted at any time, resulting in different cellular phenotypes such as empty autophagosomes due to cargo loading errors, buildup of autophagosomes

due to the inability to be trafficked or fused to the lysosome (D. D. O. Martin et al., 2015). Therefore, it is not surprising that autophagy is impaired in a myriad of diseases, ranging from neurodegeneration to cancer, and thus inspiring an aim to restore autophagy functions for therapeutic purposes. However, regulation of autophagy is incredibly complex and much remains to be understood.

1.3.2 Considerations for the potential of palmitoylation regulation in autophagy

Palmitoylation presents a promising potential means for autophagy regulation for several reasons. First, autophagy is a highly membrane-dependent process. Palmitoylation increases hydrophobicity and changes the conformation of a protein, therefore promoting membrane-membrane interactions (Chamberlain & Shipston, 2015; Linder & Deschenes, 2007). Second, palmitoylation is rapid and reversible, enabling stricter control over protein-protein or protein-membrane interactions for dynamic responses to signaling (Jiang et al., 2018; Resh, 2016; Sanders et al., 2015). Most importantly, there is already empirical evidence of several autophagy regulators that are not only palmitoylated, but whose autophagic roles are dependent on their palmitoylation as well (Kim et al., 2018; Ra et al., 2016; Sanders et al., 2019; H. Wang et al., 2015).

Only recently has evidence for the role of palmitoylation in autophagy begun to be examined, yet few studies have shown the importance of protein palmitoylation in mediating autophagy (Kim et al., 2018; Ra et al., 2016; Sanders et al., 2019). Therefore, it is important to optimize palmitoylation detection, specifically in the context of autophagy, to identify and characterize how this particular modification may influence autophagic functions, which can ultimately provide important insight in disease pathogenesis in a variety of disorders.

1.3.3 Palmitoylated proteins associated with autophagy

The most convincing argument for palmitoylation regulating autophagy is the identification and characterization of several proteins essential for autophagy which undergo palmitoylation, especially those whose autophagy functions rely on palmitoylation.

mTORC1 activation, and therefore inhibition of the autophagy initiation complex, was found to require palmitoylation (Sanders et al., 2019). Both LAMTOR1, which is critical for mTOR recruitment to lysosomes for activation, as well as mTOR, the catalytic subunit of mTORC1/2 were found to be palmitoylated (Sanders et al., 2019). Autophagy downregulation increased LAMTOR1 palmitoylation and activated mTORC1; both effects were abolished by pharmacological inhibition of palmitoylation (Sanders et al., 2019). In addition, LAMTOR1 with mutated cysteines was unable to translocate to the lysosome (Sanders et al., 2019). These findings suggest a negative regulatory role of palmitoylation in the LAMTOR/mTORC1 interaction during autophagy, in which mTORC1 activation by LAMTOR palmitoylation suppresses autophagy. However, palmitoylation in the specific regulation of the canonical mTORC signaling pathway still remains to be defined as well as its substrates.

Palmitoylation has recently been shown to regulate autophagy through another mechanism by controlling trafficking of the intracellular calcium channel mucolipin 3 (MCOLN3) (Kim et al., 2018). Intracellular trafficking of mucolipin 3, which was required for the biogenesis of the autophagosome, was shown to occur in a palmitoylation-dependent manner. Both overexpressed GFP-tagged MCOLN3, as well as endogenous MCOLN3, were found to be palmitoylated via bio-orthogonal labeling with 17ODYA and click chemistry (Kim et al., 2018). In addition, starvation-induced autophagic response increased MCOLN3 palmitoylation (Kim et al., 2018). MCOLN3 with mutated palmitoylation sites showed no increase in autophagy and was unable to traffick to autophagosomes upon starvation (Kim et al., 2018). Remarkably, palmitoylation regulation of

mucolipin trafficking and localization occurred specifically under autophagic, but not normal conditions to recruit MCOLN3 for the formation of autophagosomes (Kim et al., 2018). These findings further support a distinct, enhanced role of palmitoylation during autophagy in comparison to normal physiological conditions.

As a possible alternative autophagy mechanism in the context of pathogen removal, tripartite motif containing protein (TRIM) 31 was shown to enable autophagy related gene (ATG) 5 and 7-independent formation of autophagolysosome in a palmitoylation-dependent manner (Ra et al., 2016). Palmitoylation was found to facilitate TRIM31-mediated formation of LC3-I positive autophagolysosome originating from mitochondria by regulating TRIM31 interaction with PE, which was disabled in the presence of palmitoylation inhibitors or cysteine mutations (Ra et al., 2016). As it turns out, several TRIM family proteins influence autophagy. TRIM63 directly interacts with p62 and knockout of TRIM63 led to an upregulation of p62 while mRNA levels remained comparable (Witt et al., 2008). Interestingly, TRIM63 is predicted to be palmitoylated and may mediate selective autophagy involving p62 through palmitoylation (Blanc et al., 2015; Khan et al., 2013). Taken together, the TRIM family proteins may mediate specific autophagic pathways in response to different stimuli, but in a common palmitoylation-dependent manner, suggesting that palmitoylation in autophagy is involved in multiple pathways, further highlighting its importance in general cellular autophagy.

In addition, palmitoylation was shown to enable fusion of autophagosomes to lysosomes by mediating phosphatidylinositol (4)-kinase type 2-alpha (PI4KIIα) localization to autophagosomes, which was disabled by cysteine mutations (H. Wang et al., 2015). Preliminary data from the Martin lab has also shown several autophagy regulators to be palmitoylated with acyl-biotin exchange detection (unpublished). Strikingly, approximately 50% of all autophagy regulators have been found to be palmitoylated to date (unpublished). Taken together, the identification of a wide range of

palmitoylated proteins that are involved in autophagy suggests a widespread regulatory role of palmitoylation.

Autophagic processes do not occur through a single pathway. The identification of palmitoylated proteins in multiple autophagic pathways further underscores the importance of palmitoylation in autophagy regulation. Despite the increasing number of studies identifying and characterizing palmitoylated autophagy-associated proteins, no studies to date have aimed towards optimizing palmitoylation detection specifically in the context of autophagy on a macro scale, which will be the objective of this project.

1.4 Research objective

The objective of this study was to optimize a top-down approach of palmitoylation detection by inducing cellular autophagy, isolating and enriching palmitoylated proteins through metabolic labeling and click chemistry, and subsequent enrichment for mass spectrometry to identify proteins with changes in their palmitoylation profile. The optimization of this method may enable increased sensitivity in the detection of potential substrates of interest, particularly those implicated in diseases involving impaired autophagy, such as amyotrophic lateral sclerosis, Huntington disease, and other neurodegenerative disorders.

Chapter 2

Materials and Methods

2.1 Cell culture

Table 2.1 Mammalian cell culture

Cell line	Organism	Source
Human embryonic kidney 293T cells (HEK293T), 12022001	Human	Sigma
HeLa, epitheloid cervix carcinoma 93021013	Human	Sigma
Hippocampal derived neuronal cells (HT22)	Mouse	Michael Beazely lab

Cells were revived from frozen stocks stored at -80°C and maintained in 10 cm tissue culture plates in Dulbecco's Modified Eagle Medium (DMEM, Wisent) supplemented with 10% Fetal Bovine Serum (FBS), 1x Penicillin-Streptomycin, 2 mM L-glutamine, and 100 mM sodium pyruvate (1% vol/vol). Every 2 to 3 days or after reaching 80-90% confluency, cells were split and passaged up to approximately 30 passages. To split, cells were washed with 1X phosphate buffered saline (PBS), incubated with Trypsin-ethylenediaminetetraacetic acid (EDTA) Solution 1X (Wisent) for 5 minutes, then diluted tenfold in supplemented DMEM, and plated onto new tissue culture plates for maintenance with a further dilution factor of 5 to 20 depending on cell type and growth rate. The cells were maintained in a 37°C humidified incubator with 5% CO_2.

2.1.1 Metabolic labeling

Metabolic labeling was required for click chemistry experiments. Approximately 500,000 cells/well were plated (per 2mL of media) in 6-well tissue culture plates and grown overnight to reach 70-80% confluency. For deprivation media, DMEM was supplemented with 5% Dextran Charcoal Coated

Fetal Bovine Serum (DCC-FBS) instead of 10% FBS. Existing cell culture media was aspirated and replaced with deprivation media prewarmed to 37°C. Cells were incubated in deprivation media for 30-60 minutes depending on the protocol at 37°C prior to the addition of inhibitors, if applicable. 100 μM 2-bromopalmitate (2BP) (Sigma-Aldrich) solubilized in 100% ethanol was used as the palmitoylation inhibitor, whereas 10 μM DDD85646 (Cayman Chemical) was used as the myristoylation inhibitor. Upon addition of inhibitors, the cells were returned to 37°C for a further 15-minute incubation before addition of fatty acids.

2.1.2 Preparation and saponification of fatty acids

Alkynyl fatty acid analogs were solubilized in dimethyl sulfoxide (DMSO) (100 mM for palmitate and stearate, 25mM for myristate) and stored at -20°C. If applicable, alkyne-labeled and unlabeled fatty acids were saponified with 20% molar excess of KOH in 1:1 ratios in 3 mL glass reaction vials and incubated at 65°C for 5 minutes, or until no solids remain. Immediately after, 50 volumes of 20% fatty acid free bovine serum albumin (FAFBSA) prepared in unsupplemented DMEM and pre-warmed to 37°C were added to the saponified fats such that the volume ratio was 1:1:50 of fatty acid:KOH:FAFBSA (Table 2.2). The fatty acid mixture was incubated for at least 15 minutes at 37°C. Appropriate volumes of saponified or non-saponified fatty acids were added dropwise to cells (Table 2.2). The cells were then returned to incubate at 37°C for 2-4 hours for labeling, depending on the experimental condition. After labeling, cells were harvested in lysis buffer and collected.

Table 2.2 Saponification of fatty acid solution ratios and volumes

Total media volume (mL)	Vol. fatty acid or fatty acid analog (μL)	Vol. KOH (μL)	Vol. 20% FAFBSA (μL)	Total vol. of saponified label to add to cells (μL)
4	4	4	200	208
2	2	2	100	104

(Liao et al., 2021)

2.1.3 Calcium phosphate transfection

For studies involving a specific protein of interest, HEK293T cells were transfected with the DNA via calcium phosphate DNA coprecipitation, as previously described (Jordan et al., 1996). Briefly, cells were grown to 60-80% confluency in 6-well tissue culture plates and a DNA mix was added dropwise to the media. The DNA mix consisted of 20 µL DNA (5 µg), 10.2 µL $CaCl_2$ (2 M), 53.1 µL molecular grade distilled deionized H_2O (ddH_2O), and 83.3 µL 2X 4-(2-hydroxyethyl)-1-piperazineethanesulfonic acid (HEPES) buffered saline (HBS). 2 hours after addition of the DNA mix, cell culture media with the DNA mix were removed and replaced with fresh media. Cells were typically transfected for 18-20 hours prior to downstream biochemical applications.

Table 2.3 List of DNA plasmids used for transfection in HEK293T cells

DNA Construct	Reference	Source
G2A-HTT-GFP	(D. D. O. Martin et al., 2014)	Gift from Bertiaume lab
SVIP-mCherry	N/A	Martin lab
myr-HTT-GFP	(D. D. O. Martin et al., 2014)	Gift from Bertiaume lab
Spike-mCherry	(Gordon et al., 2020)	N/A
zDHHC17-HA	(Holland et al., 2016)	Gift from Thomas lab

2.1.4 Induction of autophagy

HeLa cells were used for experiments involving autophagy induction. Autophagy was pharmacologically induced with rapamycin (solubilized in EtOH, Millipore) at 200 nM final concentration. In some samples, 100 nM bafilomycin A1 was also added with rapamycin to prevent degradation of the autophagosome, thus allowing the detection of the autophagy marker proteins.

2.1.5 Lysis

Following aspiration of media and one wash with 1X PBS, the cells were harvested and lysed on ice. A modified radioimmunoprecipitation assay (RIPA) buffer (0.1% SDS, 50 mM N-2-hydroxyethylpiperazine-N-ethanesulfonic acid (HEPES) pH 7.4, 150 mM NaCl, 1% Igepal CA-630, 0.5% sodium deoxycholate, 2 mM $MgCl_2$ with freshly added 1 mM phenylmethylsulphonyl fluoride (PMSF) and 10 µg/µL Pepstatin A (or EDTA-free complete protease inhibitor cocktail CIP)) was used for the lysis of metabolically labeled cells. In the case of click chemistry detection, metal chelating agents such as EDTA were avoided in the lysis buffer to prevent inhibition of the click chemistry reaction via removal of copper ions (Kit & Martin, 2019; Presolski et al., 2011). Between 0.5-1 mL of lysis buffer was used per 2-4 mL of cell culture media. Following addition of lysis buffer, cells were scraped off with a cell scraper and the lysates were collected in pre-chilled 1.5 mL microcentrifuge tubes. The lysates were then incubated at 4°C rotating end-over-end for 15 minutes, prior to centrifuging at 16,000 xg for 10 minutes at 4°C. The supernatant was collected into fresh 1.5 mL microcentrifuge tubes for further analysis or stored at -20°C until needed.

The concentration of proteins following lysis was determined using a detergent compatible (DC) assay as per manufacturer's instructions (BioRad), using 1 mg/mL bovine serum albumin (BSA) as the protein concentration standard.

2.2 Immunoprecipitation

Equal amounts of proteins were transferred to new tubes and immunoprecipitated at 4°C rocking overnight with 0.5-1 µL of primary antibody.

Protein G beads (magnetic or sepharose) were equilibrated 3 times with lysis buffer or the same buffer as the protein samples, and resuspended. 20-30 µL of the beads slurry were added to each sample and rocked at 4°C for 2-3 hours. Following incubation, the beads were washed 3 times with

the previous buffer and resuspended in 45 µL 1% SDS (50 mM HEPES, pH 7.4), followed by heating at 80°C for 15 minutes with intermittent mixing. Typically, 43 µL of the eluted proteins are used for click chemistry right away.

2.3 Click chemistry detection

Stock solutions of click chemistry reagents were prepared at appropriate concentrations. 2 mM Tris-(benzyltriazolylmethyl) amine (TBTA) was solubilized in DMSO and stored under N_2 gas to prevent oxidation. 50 mM CuSo4 was solubilized in ddH2O and stored at room temperature. 250 mM Tris-carboxyethylphosphine-HCl (TCEP-HCl) was solubilized in ddH2O and stored at 4°C protected from light. TCEP-HCl was diluted to 50 mM fresh when needed. Azido probes, including biotin azide, Dde biotin azide plus, and AFDye 647 fluorescent azide plus, were solubilized in DMSO and diluted to 2 mM and stored at -80°C under N2 gas in small aliquots.

The click chemistry master mix was prepared by adding thawed reagents in the following order in volumes specified in Table 2.4: TBTA, $CuSO_4$. TCEP-HCl, azido probe. The master mix was well-mixed before addition to protein samples.

Click chemistry can be performed on either total protein lysates, or immunoprecipitated proteins. The protein samples were made up to 1% SDS to increase accessibility of the click chemistry reagents. The samples following addition of the click master mix were thoroughly mixed. The samples were reacted at 37°C for 30 minutes in darkness, with intermittent mixing by agitation. Following the 30-minute incubation, the reaction was stopped either by precipitation with 10 volumes of ice cold 100% acetone, or through denaturation with sample loading buffer (SLB) (BioRad) to 1X concentration with β-mercaptoethanol (βme) or dithiothreitol (DTT). Final concentrations of the reducing agents were kept below 20-25 mM to avoid hydrolyzing the thioester bonds and consequent

loss of signal. The denatured sample in SLB was boiled at 95°C for 5 minutes prior to separation by SDS-PAGE.

Table 2.4 Click reagent and protein volume ratios

Total reaction mix vol. (µL)	Vol. protein (µL)	Vol. TBTA (2 mM) (µL)	Vol. CuSO4 (50 mM) (µL)	Vol. TCEP (50 mM) (µL)	Vol. azido probe (2 mM) (µL)
50	43	2.5	1	1	2.5
100	86	5	2	2	5

(Liao et al., 2021)

2.4 Biotin-based enrichment following click chemistry

For enrichment of proteins, the click chemistry reaction volumes were multiplied 10-fold in 15 mL Falcon tubes to provide enough protein. The reaction was stopped by precipitating the proteins with 10 volumes of ice-cold acetone overnight. The next day, the precipitated proteins were spun down at 3000 rpm at 4°C for 3 minutes, and excess acetone was decanted and allowed to evaporate for 5 minutes.

The protein pellet was thoroughly resuspended and transferred to 1.5 mL microcentrifuge tubes. Depending on the experiment, either the aforementioned RIPA lysis buffer or the ABE lysis buffer (50 mM HEPES, 2% SDS, fresh protease inhibitors without EDTA) was used to resuspend the protein pellet. Prior to the addition of beads, 50 µL of clicked proteins were saved as input. 20-30 µL of pre-equilibrated high capacity magnetic streptavidin (Click Chemistry Tools) or high capacity neutravidin Sepharose beads (Thermo) were added to the samples. The samples were then incubated 2-3 hours end-over-end at 4°C.

Following incubation, the beads were briefly spun down and washed 3 times in the same buffer the proteins were resuspended in.

2.4.1 ABE-based elution of proteins following acetone precipitation of clicked proteins

The precipitated protein pellet was thoroughly resuspended in 0.5 mL ABE lysis buffer. ABE dilution buffer was prepared (50 mM Tris pH 7.0, 1% Triton x 100, 1 mM EGTA, protease inhibitors, and NaCl as needed). To each sample, 9.5 mL of ABE dilution buffer (150 mM NaCl) were added. 30 µL of beads (pre-equilibrated 3 times in dilution buffer with 150 mM NaCl) was added to each sample and incubated end-over-end at 4°C for 3 hours.

The samples were spun down at 1800 rpm for 3 minutes at 4°C and the supernatant was decanted. The beads were then resuspended in 1 mL dilution buffer (500 mM NaCl) and transferred to microcentrifuge tubes. The beads were washed twice more in dilution buffer (500 mM NaCl) and then an additional 2 times in dilution buffer (no NaCl).

The samples were eluted in 60 µL of ABE dilution buffer containing additional reagents (0.2% SDS, 250 mM NaCl, 1% βme) at 37°C for 10 minutes with flick-mixing. Both the eluted samples and input were denatured in SLB (1x final concentration) with 20 mM β-me and boiled at 95°C for 5 minutes before electrophoresis.

2.5 SDS-PAGE and western blotting

2.5.1 Electrophoresis and transfer

Denatured proteins were separated on 10-12% tris-glycine or bis-tris acrylamide gels through electrophoresis. Samples were loaded into the wells along with 3-5 µL Precision Plus Protein Standards (BioRad). Tris-glycine gels were run in 1X Tris-glycine-SDS running buffer (BioRad), whereas bis-tris gels were run in 1X MOPS (3-(N-morpholino) propanesulfonic acid) buffer (BioRad). The gels were run at between 120-160V.

For western blotting, nitrocellulose or methanol-activated PVDF membranes were equilibrated in 1X transfer buffer (BioRad). Following electrophoresis, the proteins were transferred onto the membranes for 25 minutes with limit 25 V, constant 1.0 A using the semi-dry Transblot Turbo apparatus (BioRad). To reduce background, the membranes were blocked in 5% skim milk blocking buffer in PBS-T (1X PBS, 0.1% Tween 20) rocking for 1 hour at room temperature, or overnight at 4°C.

As an extra control to confirm the presence of thioester bonds in palmitoylated proteins, the membranes can undergo an alkali treatment to hydrolyze the thioester or ester bonds. In this case, samples were loaded into 2 duplicate protein gels for separation and transferred onto separate PVDF membranes. Following electrophoresis and a few rinses of both membranes with ddH_2O, the membranes were treated before the addition of blocking buffer. One membrane was treated with 5 mL 0.1M KOH in 90% methanol, while the second duplicate was treated with 5 mL of 0.1M Tris (pH 7.0) in 90% methanol as a control. The membranes were treated for 1 hour rocking gently at room temperature, followed by 6 washes in PBS-T. The membranes were then blocked in 5% skim milk blocking buffer.

2.5.2 Probing with antibodies

Primary antibodies were diluted in 5% skim milk blocking buffer and added to membranes, and incubated rocking at 4°C overnight. The membranes were then washed 4 times in PBS-T (5 mins each). Secondary antibodies, including those specific for housekeeping proteins as loading control, were diluted in 5% bovine serum albumin (BSA) in PBS-T with 0.01% SDS and added to each membrane for 1 hour, rocking gently at room temperature protected from light. Following 4 washes in PBS-T (5 mins each), the membranes were visualized with the ChemiDoc imager (BioRad).

Table 2.5 List of primary antibodies

Name/antigen	Host Species	Method (western/IP)	Dilution	Source
α-GFP	Goat	IP	1:5000	Biolegend
α-GFP	Rabbit	western	1:5000	Biolegend
α-HA	Rat	IP	1:1000	Biolegend
α-HA	Mouse	western	1:1000	Biolegend
α-LC3I/II	Rabbit	western	1:1000	Cell Signaling
α-mCherry	Mouse	IP/western	1:5000/ 1:2500	Biolegend
α-mCherry	Rabbit	IP/western	1:1000/ 1:1000	Cell Signaling
α-p62	Rabbit	western	1:1000	Cell signaling

Table 2.6 List of secondary antibodies

Name	Excitation/ Emission	Raised in	Against	Dilution	Source
Alexa Fluor 488	488/519	Donkey /goat	Rabbit	1:2500	Life Technologies
Alexa Fluor 555	555/567	Donkey	Mouse	1:5000	Invitrogen
Anti-tubulin hFAB rhodamine	530/580	N/A	Tubulin	1:5000	BioRad
Anti-GAPDH hFAB rhodamine	530/580	N/A	GAPDH	1:5000	BioRad
Alexa Fluor Streptavidin 680 Conjugate	680/706	N/A	Biotin	1:5000	Invitrogen
StarBright Blue 520	440/520	Goat	Rabbit	1:2500	BioRad

Chapter 3

Optimization of Click Chemistry Detection

Metabolic labeling in combination with click chemistry detection is a rapid and sensitive method to detect protein palmitoylation, in comparison to alternative exchange-based methods. Therefore, large-scale identification of palmitoylated and myristoylated proteins are possible through mass spectrometry, as well as further downstream applications with additional techniques such as pulse-chase analysis of dynamic palmitoylation and affinity-based enrichment (Gao & Hannoush, 2017; B. R. Martin et al., 2012; B. R. Martin & Cravatt, 2009). Compatible with a variety of cell types and even live animal models (Hong et al., 2010; Yap et al., 2010), click chemistry is a versatile and powerful tool for the study of protein palmitoylation. However, click chemistry is not without limitations. The assay itself is fastidious and can involve a considerable amount of troubleshooting. In addition, traditional routes of fatty acid analog delivery into cells may be problematic. Most protocols for metabolic labeling involve adding fatty acids directly to cell culture media, which poses several issues (Blanc et al., 2015). Firstly, fatty acids, especially those with longer hydrocarbon chains, are very insoluble (Blanc et al., 2015), which directly impacts their incorporation from cell culture media. In addition, direct addition of fatty acids to cell culture can lead to lipotoxicity, therefore affecting the viability of the cells and interfering with experimental results by activating unwanted pathways including ER stress and ceramide-mediated apoptosis (Alsabeeh et al., 2018; Z. Li et al., 2008; Listenberger et al., 2001; Yin et al., 2015). Therefore, these existing issues in addition to continuing development of new tools and reagents provide opportunities to optimize click chemistry detection.

The aim of the following set of experiments is to optimize click chemistry detection by improving fatty acid delivery during metabolic labeling, as well as testing several click chemistry reagents

including biotin-based and fluorescent azido probes to lay the groundwork for the isolation and purification of palmitoylated proteins during autophagy.

3.1 Testing and optimization of click chemistry reagents and detection

Since the development of click chemistry detection of fatty acylation, an increasing number of new reagents have become commercially available, with varying degrees of efficacy. Therefore, we sought to test several click chemistry tools from different suppliers and examined the stability of biotin azide in particular by comparing new and old stock solutions stored at -20°C.

Tris-(benzyltriazolylmethyl) amine (TBTA) provides the ligand for the click chemistry reaction and is therefore an important reagent (Yang et al., 2014). We compared two structurally identical products from Cayman Chemical and Click Chemistry Tools (CCT) solubilized in DMSO with different storage conditions, which could affect stability. Total myristoylation was detected by detecting biotin conjugated to myristoylated proteins through the click chemistry reaction between the alkyne and azido groups. Overall, both TBTAs yielded comparable myristoylation signals, suggesting equivalent ligation efficiency (Figure 3.1).

In addition, biotin-based azido probes were solubilized in DMSO and compared. To test for stability of the reagent and whether binding efficiency decreases over time in storage, freshly made 2 mM biotin azide stock solutions and older stock solutions that were stored at -20°C were compared, as well as Dde biotin azide plus. Azide plus products from Click Chemistry Tools possess a complete copper-chelating system included in its structure, capable of rapidly forming copper complexes that aim to drastically increase the reaction kinetics by increasing copper concentration (proprietary product from Click Chemistry Tools) as well as stabilize the copper oxidation state to reduce toxicity to enable live cell labeling conditions (Hong et al., 2010). Therefore, Dde biotin azide plus is expected to yield increased overall signal from the click chemistry reaction. In addition, Dde contains

a spacer arm that is hydrazine cleavable, which presents an option in the future for downstream enrichment processes.

To compare the click chemistry reagents, HEK293T cells were labeled with alkynyl myristate or myristate (no alkyne) as a control. One fatty acid is sufficient for the purpose of comparing reagents for click chemistry, therefore myristate was used since it is the most soluble fatty acid in comparison to palmitate or stearate, and consequently improves the efficiency of the experiment. The preliminary results suggested a slight increase in total myristoylation signal with Dde biotin azide plus, in comparison to both biotin azide stock solutions (Figure 3.1A).

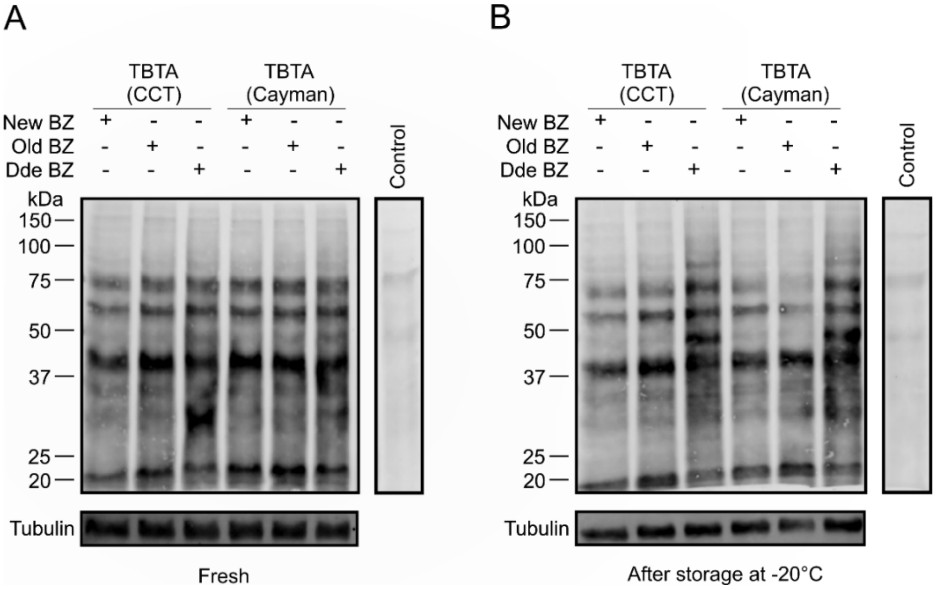

Figure 3.1 Comparison of total myristoylation signal using biotin azide and Dde biotin azide plus over storage time of click samples.

HEK293T cells were labeled with alkynyl myristate or unlabeled myristate (control) and the protein lysates subjected to click chemistry with different reagents, including two TBTAs from Click Chemistry Tools (CCT) and Cayman Chemicals. Biotin azide stock solutions stored for 2 months at -20°C, freshly made biotin azide, and Dde biotin azide plus were compared. The control samples were subjected to the same detection conditions on the same blot. Half of the clicked samples was subjected to immediate SDS-PAGE separation (A), while the other half was stored at -20°C for 3 days prior to SDS-PAGE separation (B). Total myristoylation was detected using Alexa Fluor Streptavidin 680 Conjugate (Invitrogen). Tubulin was used as a loading control; anti-tubulin rhodamine (1:5000). The blots were scanned separately, and the figure represents composite images of the same blot.

Next, to test the stability of protein lysates that underwent the click chemistry reaction (hereafter referred to as "clicked"), half of the same samples were stored at -20°C following denaturation with sample loading buffer and detected by western blot 3 days later. Biotin azide samples appear to have lost some myristoylation signal after freezing (Figure 3.1A and B). However, Dde biotin azide plus clicked samples showed no decrease in myristoylation when comparing frozen to fresh samples (Figure 3.1 compare Dde BZ panels between A and B), and the myristoylation signal was also noticeably stronger than the biotin azides. The preliminary data suggested that Dde biotin azide plus may provide a more stable biotin signal in comparison to biotin azide if samples need to be stored and

cannot be processed immediately. Unlabeled myristate (no alkyne group) was included as a control in click chemistry. Although minimal, there was some background detected of endogenously biotinylated proteins that were not as a result of the click chemistry reaction.

3.1.1 Fluorescent azido probes

To explore an additional method to detect proteins and avoid the detection of background biotinylated proteins, we sought to acquire alternative detection methods using fluorescently-tagged azido probes, which allow in-gel imaging without the transfer of proteins onto a membrane. For this, we utilized the AFDye 647 azide plus from Click Chemistry Tools, which is structurally similar and almost spectrally identical to the commonly used Alexa 647 (proprietary product of Click Chemistry Tools). In addition, this fluorescent azide is also an "azide plus" reagent which structurally includes the copper-chelating system mentioned earlier. Previously, clicked palmitoylated or myristoylated proteins were conjugated to biotin through the click chemistry reaction, and detection was achieved indirectly by detecting biotin with fluorescent streptavidin. With the AFDye 647 azide plus, we were able to bypass biotin and directly detect the fluorescent azide linked to fatty acid-modified proteins through the click chemistry reaction. This approach excludes endogenously biotinylated proteins in the background and improve signal-to-noise ratio.

Alkynyl palmitate was used to label HEK293T cells with unlabeled palmitate (no alkyne group) as a negative control for click chemistry. With the exception of the azido probes, the remaining click chemistry reagents were consistent between the samples. The preliminary results showed that fluorescent azides provide a clean visualization of alkyne labeled fatty acids with click chemistry, with no background detection of biotinylated proteins when using unlabeled fatty acids (no alkyne), which was present when biotin-based probes were used (Figure 3.1 controls). Visualization was

optimized when scanned in-gel. The fluorescent azide effectively improved signal-to-noise ratio and eliminated detection of any biotinylated proteins that did not result from click chemistry linkage.

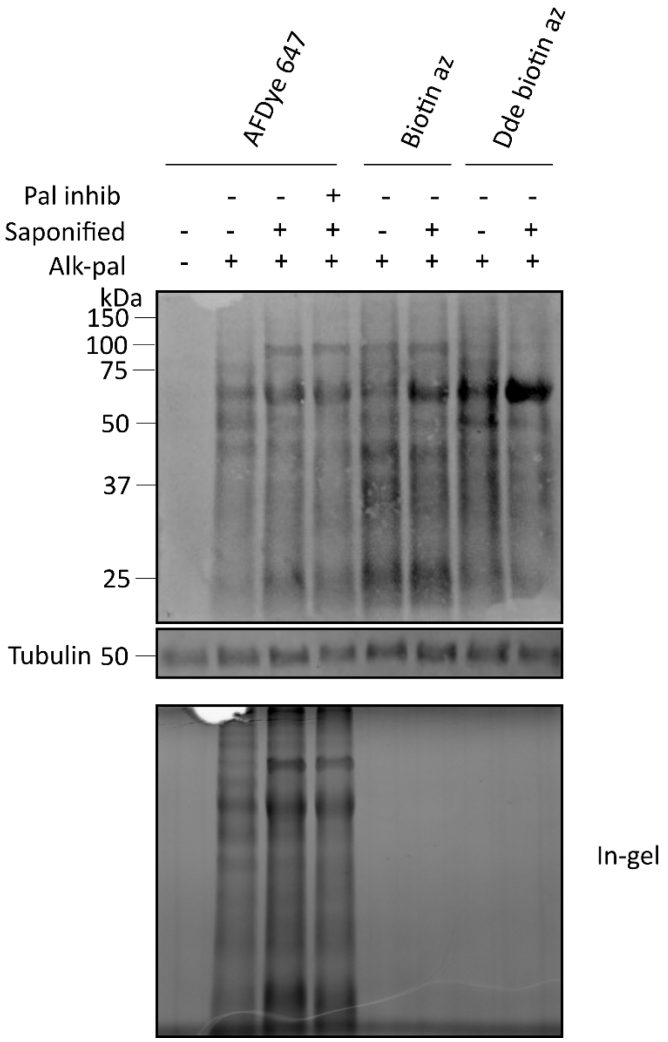

Figure 3.2 Comparison of total palmitoylation signal using biotin azide, Dde biotin azide plus, and fluorescent AFDye 647 azide plus in clicked protein samples.

Total protein lysates were clicked with either 2 mM AFDye 647 fluorescent azide plus, biotin azide, or Dde biotin azide plus (solubilized in DMSO). Top blot represents overall palmitoylation detected using Alexa Fluor Streptavidin 680 Conjugate (Invitrogen) on PVDF membrane and scanned at Alexa 680 detection for the biotin signal. Bottom represents the in-gel image scanned at Alexa 647 before transfer onto PVDF membrane for direct detection of the fluorescent palmitoylation signal. 100 µM of 2-bromopalmitate was used as a general palmitoylation inhibitor. Tubulin was used as a loading control; anti-tubulin rhodamine (1:5000).

In addition to azido probes, alkynyl palmitate (alk-pal) was either added directly to media or saponified and incubated in fatty acid-free BSA, as described in Chapter 2. The preliminary results showed a stronger palmitoylation signal as well as the detection of additional bands when alk-pal was saponified across all azido probes (Figure 3.2). However, 2BP did not seem to have any inhibitory effect on the saponified alkyne palmitate-labeled samples. The effect of saponification in improving palmitoylation detection is discussed in detail in Section 3.2.

The fluorescent azide provided clean images and reduced background of endogenously biotinylated proteins. However, proteins clicked with AFDye 647 azide plus did not transfer as well as samples clicked with biotin-based azido probes. In addition, this approach required alternative means to confirm equal loading across lanes. Another drawback of fluorescence-based detection is the inability to perform an in-gel alkali treatment to confirm the presence of thioester bonds, and verifying protein palmitoylation as opposed to other forms of lipidation such as N-myristoylation. This approach was shown to be sensitive and convenient for in-gel visualization and quantification, as well as western blotting if the transfer of proteins clicked with fluorescent azides onto membranes were improved.

3.1.2 Additional steps for click chemistry detection

To bypass the necessity of transferring proteins to membranes to perform the necessary controls, we explored alternative means to quantify loading controls and perform alkali treatments.

Coomassie blue staining of protein gels were performed and was shown to be a good alternative to ensure equal loading by quantifying total protein signal per lane, as opposed to probing for a housekeeping protein once transferred to a membrane (data not shown).

Alkali treatment to hydrolyze thioester bonds, thereby providing further validation of S-acylation, is often necessary. This additional step differentiates myristoylated and palmitoylated proteins. The most common method involves treating proteins transferred to PVDF membranes with 0.1M KOH in

90% methanol for 1 hour, which is sufficient to hydrolyze thioester bonds and consequently remove the palmitoylation signal, whereas the myristoylation signals remain due to the alkali-resistant amide bond. However, this is not suitable for the treatment of gels. Another possible method is to treat with hydroxylamine (HAM) in-gel, which cleaves thioester bonds and de-acylates proteins (Drisdel et al., 2006). This treatment was previously shown to remove S-acylation signals (Kostiuk et al., 2008). However, the attempt to replicate the protocol was not successful as in-gel HAM treatment failed to remove any S-acylation signal from samples clicked with fluorescent azides (data not shown). Therefore, the Tris/KOH treatment on PVDF membranes remains the only functional method to hydrolyze thioester bonds and confirm S-acylation.

3.1.3 Types of gels for separation

Once we achieved clean and robust palmitoylation signals using fluorescent azides, we aimed to optimize downstream detection following the click reaction, especially because alternative methods for in-gel alkali treatments were unsuccessful. First, in an attempt to improve protein transfer for western blotting, we tried bis-tris gels as opposed to tris-glycine protein gels. Tris-glycine gels did not transfer well and showed a considerable loss of protein (Figure 3.2 top) despite lowering the concentration of polyacrylamide from 12% to 10% (data not shown). 10% bis-tris gels showed better protein separation with more distinct bands, although the gel images were not quantifiable due to consistent saturation in the control lanes of non-alkynyl fatty acids (data not shown). However, bis-tris gels transferred more efficiently under the same settings, and therefore was established as the standard gel to separate clicked protein samples.

3.2 Optimization of fatty acid delivery during metabolic labeling

Our most important optimization for click chemistry detection of S-acylated proteins, as well as N-myristoylated proteins, was achieved by establishing a protocol for improved metabolic labeling

using delipidated media and saponified fatty acids incubated in fatty acid-free bovine serum albumin (FAFBSA), which was recently published in the Journal of Visual Experiments (Liao et al., 2021). Current general protocols in the field involve direct addition of fatty acid analogs to cell culture media, which can limit cellular uptake of the label due to insolubility, leading to significant impediments to the sensitivity of downstream click chemistry detection. In addition, direct addition of free fatty acids into cells can activate unwanted stress pathways (Listenberger et al., 2001; Yin et al., 2015).

3.2.1 Types of media for labeling

Most metabolic labeling studies of fatty acylated proteins to date involve direct addition of fatty acids to regular cell culture media, which already contains fatty acids. This may lead to competition between alkynyl fatty acid analogs and endogenous fatty acids for proteins to utilize for lipidation modifications such as S-acylation or N-myristoylation, and therefore reduce cellular incorporation and the fatty acylation signal. The purpose of using delipidated media is to provide cells with only alkynyl fatty acid analogs for lipidation, thereby increasing incorporation of the analogs. This was achieved by supplementing Dulbecco's Modified Eagle Medium (DMEM) with dextran charcoal-coated fetal bovine serum (FBS) (referred to hereafter as delipidated media), which strips off non-polar materials such as fatty acids that are present in regular FBS. Therefore, delipidated media encourages cells to use alkynyl fatty acids instead of endogenous fatty acids.

I tested the effect of using delipidated media versus regular media. HEK293T cell culture media was replaced with either fresh regular DMEM or delipidated DMEM prior to the addition of alkynyl stearate. Either non-saponified or KOH saponified alkynyl-stearate in FAFBSA was added to cells and click chemistry was performed on total protein lysates with AFDye 647 azide plus. The preliminary results showed that with the addition of non-saponified alkynyl stearate, delipidated

media with DCC-FBS exhibited an increase in protein S-acylation signal, relative to the non-saponified label in regular media (Figure 3.3). However, when the fatty acid was saponified and incubated in FAFBSA, there was no difference in S-acylation signal between delipidated and regular media (Figure 3.3), suggesting that depriving cells of endogenous fatty acids was more effective at improving S-acylation signal when the label was added directly to the media in which it dissolves poorly.

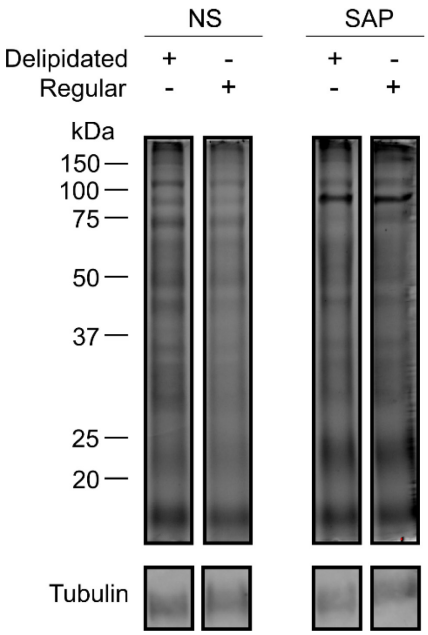

Figure 3.3 Comparison of S-acylation detection in regular versus delipidated media using saponified or non-saponified alkynyl-stearate.

HEK293T cells were labeled with non-saponified (NS) or saponified alkynyl-stearate in FAFBSA in either regular (5% FBS) or delipidated media (5% DCC-FBS). Total protein lysates were clicked with AFDye 647 azide plus and visualized directly on tris-glycine protein gel. Tubulin was used as a loading control after transfer to PVDF membrane; anti-tubulin rhodamine (1:5000).

Next, we examined the difference between the traditional labeling technique of direct addition of fatty acid to regular media, and the addition of saponified fatty acids in FAFBSA to delipidated media.

3.2.2 Saponification of fatty acids

Long chain fatty acids are generally insoluble, which is exacerbated with increasing number of carbons in the hydrocarbon chain. By saponifying fatty acids with a molar excess of potassium hydroxide (KOH), the fatty acid salt becomes less toxic. In addition, incubation in bovine serum albumin (BSA), a carrier protein, will further improve incorporation into the cell. The effect of saponification was first explored by Yap and colleagues, however, the authors stated that saponification of the fatty acids yielded comparable results to non-saponified fatty acids (Yap et al., 2010). Our findings were contradictory. Therefore, we aimed to demonstrate the effect of saponification on the delivery of fatty acid analogs, as well as establish saponification methods in the Martin lab. To avoid interfering with fatty acid incorporation, fatty acid-free BSA (FAFBSA) was used. Three alkynyl fatty acids (alkynyl myristate (13-TDYA), alkynyl palmitate (15-HDYA), and alkynyl stearate (17-ODYA)) were saponified with a 20% molar excess of KOH and incubated in FAFBSA. These modifications were predicted to have the greatest effect on stearate, which has the longest hydrocarbon chain out of the three and is therefore the most insoluble. Conversely, saponification was not predicted to have a significant effect on myristate, which is more soluble due its shorter chain length. Unexpectedly, saponifying alkynyl myristate led to a significant decrease in the total myristoylation signal when compared to the non-saponified samples (Figure 3.4 left). On the other hand, saponification noticeably increased fatty acylation signal of alkynyl palmitate, but yielded the most significant increase in alkynyl stearate (Figure 3.4 middle and right). This suggested an overall increase in cellular uptake of the alkynyl fatty acids that are used for palmitoylation during metabolic labeling. Although the increase in saponified alkyne palmitate was insignificant when compared to non-saponified, a change in the banding pattern was observed in which some bands in particular showed a much more robust increase in acylation signal in the saponified treatment (Figure 3.4 middle). In addition, alkynyl myristate was resistant to KOH treatment, as expected, since

myristate undergoes N-myristoylation through an alkali-resistant amide bond, as opposed to palmitate and stearate, both of which undergo S-palmitoylation through a thioester bond that is alkali-sensitive. Consistent with palmitoylation, treatment with KOH largely removed the fatty acids from proteins modified with both alkynyl palmitate and alkynyl stearate, confirming that the majority of the signal was through a thioester or ester bond (Figure 3.4 compare top and bottom panels).

Similarly, we investigated whether saponification has a similar effect on 2-bromopalmitate (2BP), the general S-acylation inhibitor, since it is also a fatty acid analog. We found that saponifying 2BP in samples labeled with saponified alkynyl palmitate or stearate, did not affect acylation levels when compared to samples treated with non-saponified 2BP in total protein lysates subjected to click chemistry (data not shown).

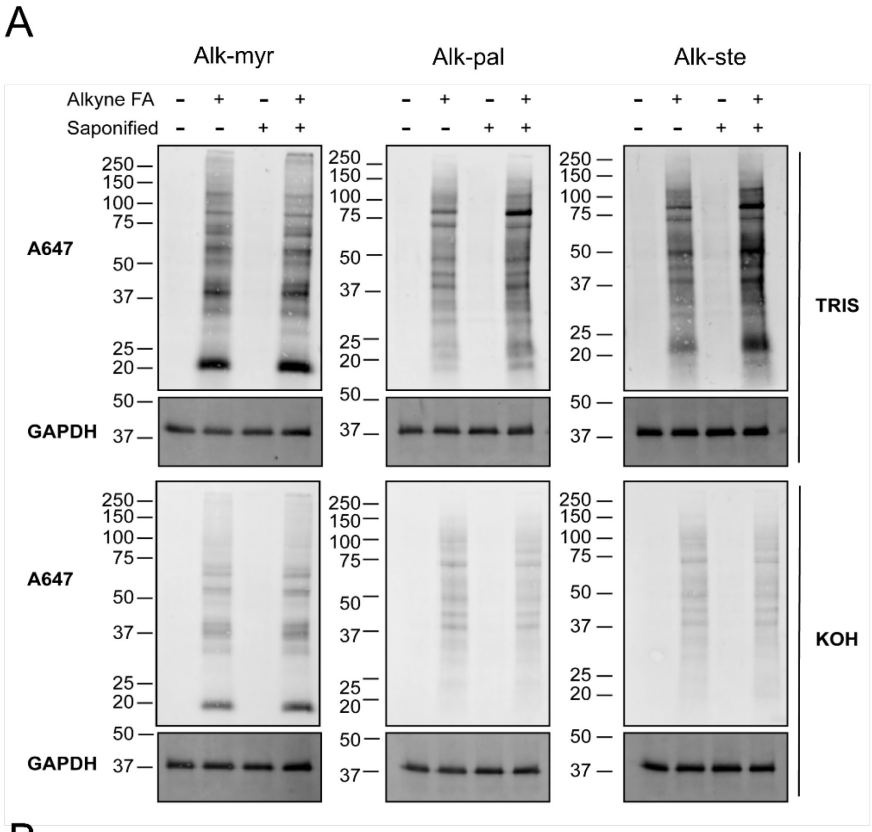
A
Alk-myr
Alk-pal
Alk-ste
Alkyne FA
Saponified
A647
GAPDH
TRIS
KOH
250
150
100
75
50
37
25
20
B
Arbitrary units of total acylation signal normalized to GAPDH
*
ns
non-saponified
saponified
Alk-myr
Alk-pal
Alk-ste

Figure 3.4 Saponification of alkynyl fatty acids yields changes in the overall fatty acylation signal in HEK293T cells using click chemistry.

A) HEK293T cells were labeled with the indicated fatty acids either directly into cell culture, or following saponification. Alkynyl fatty acid-modified proteins were linked to AFDye 647 azide plus, and separated via SDS-PAGE in duplicate before transfer to PVDF. After treatment with either 0.1M Tris pH 7.0 (top) or 0.1M KOH (bottom) to hydrolyze thioester bonds, fatty acylation was detected at 647nm excitation. Unlabeled (no alkyne group) fatty acids were used as negative controls for click chemistry. GAPDH was used for loading control (anti-GAPDH rhodamine. 1:5000). B) Total acylation signal of non-saponified samples vs. saponified samples, normalized to GAPDH, were shown as the mean + SEM (paired T-test, * indicates $p \leq 0.05$, n=3). Figure is representative of results using two different detection methods involving both biotin and fluorescent azides. Modified from Liao et al., 2021.

3.2.3 Optimized fatty acid delivery in HT22 cells

To demonstrate the versatility of metabolic labeling, as well as a global increase in fatty acylation signal with delipidated media and saponified fatty acids in FAFBSA, the same saponification experiment was performed in HT22 cells. In addition, the mouse HT22 cells are hippocampal-derived. Since we are particularly interested in palmitoylation during autophagy in the brain, the HT22 cells would provide a more relevant picture. The cells were labeled in the same manner as mentioned above. Similar to the HEK293T cells, the preliminary results showed that our labeling approach noticeably increased palmitoylation signal in cells labeled with alkynyl stearate (Figure 3.5 right). There was no effect of saponification and delipidated media in alkynyl myristate (Figure 3.5 left), consistent with data from HEK293T cells shown in Figure 3.4. Although no noticeable change was observed in the alkynyl palmitate samples (Figure 3.5 middle), we also observed different banding patterns in the saponified samples in that some bands became robustly acylated in comparison to the rest of the lane, consistent with HEK293T cells (Figure 3.4 and 3.5 middle panels). Quantification of fatty acylation signals showed the same trend as in HEK293T cells represented in Figure 3.4. Comparable to HEK293T cells, 13-TDYA labeled proteins were KOH-resistant, while both 15-HDYA and 17-ODYA showed susceptibility to KOH with a significant loss of fatty acylation

signal. Although DDD85646 showed noticeable inhibition of N-myristoylation with 13-TDYA (Figure 3.5 left), 2BP did not affect the detection of acylated proteins with 15-HDYA nor 17-ODYA, which have mostly undergone S-acylation, confirmed by loss of signal following alkali treatment (Figure 3.5 middle and right). Only proteins labeled with non-saponified 15-HDYA seemed to show a mild decrease in acylation signal when 2BP was present, but not proteins labeled with 17-ODYA. Similar inhibitory effects were observed in HEK293T cells as well (Figure 3.2). Therefore, 2BP may not be an ideal palmitoylation inhibitor.

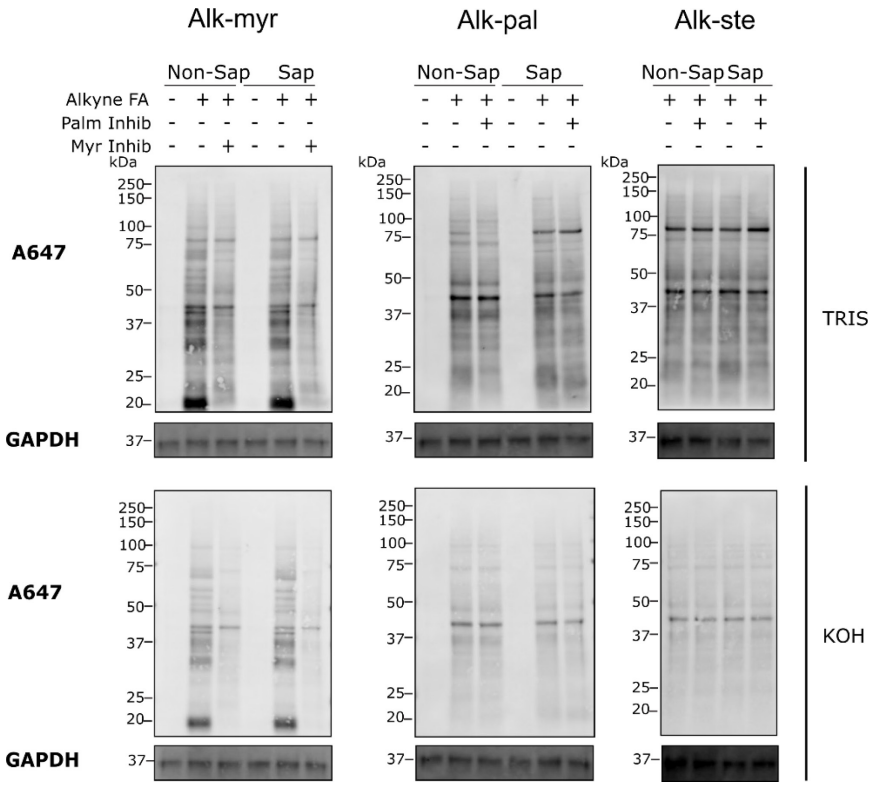

Figure 3.5 Saponification of alkynyl fatty acids yields changes in the overall fatty acylation signal in mouse HT22 cells using click chemistry.

HT22 cells were labeled with the indicated fatty acids added either directly into cell culture media, or following saponification. Where indicated, 100 μM 2BP or 1 μM DDD85646 was added to inhibit palmitoylation (palm inhib) or myristoylation (myr inhib), respectively . Alkynyl fatty acid-modified proteins were linked to AFDye 647 azide plus, and separated via SDS-PAGE in duplicate before transfer to PVDF. After treatment with either 0.1 M Tris pH 7.0 or 0.1M KOH to hydrolyze thioester bonds, fatty acylation was detected at 647nm excitation. Unlabeled (without alkyne group) fatty acid were used as a negative control for click chemistry. GAPDH was used for loading control (anti-GAPDH rhodamine; 1:5000).

The preliminary HT22 results show that our optimized approach for metabolic labeling using delipidated media, as well as saponified fatty acids incubated with FAFBSA, can improve fatty acylation, particularly S-acylation signal using stearate, and amplify detection of S-acylated proteins in a variety of cell lines.

3.3 Summary and discussion of results

In these experiments, we have tested biotin as well as fluorescent azido probes. Fluorescent azides are easy to visualize through direct in-gel imaging, eliminating the transfer to membranes and any resulting loss of protein for western blotting if only interested in total or overall protein palmitoylation/myristoylation in the cells during the labeling period. However, fluorescent azides can only be used for visualization, and cannot be used for further downstream applications such as affinity purification. On the other hand, biotin-based azido probes are also sensitive and can enable further enrichment using avidin. Variations of biotin azides, such as the Dde biotin azide plus with a hydrazine-cleavable linker provides additional options for eluting proteins and may also increase stability of the palmitoylation/myristoylation signal, as the data suggests (Figure 3.1). On initial examination, the copper-chelating system present in azide plus does not seem to increase detection of fatty acylation, but may increase the stability of the click chemistry linkage. The copper-chelating component increases the rate of the click chemistry reaction and enables almost immediate linkage between the alkyne and the azide plus reagent; however, this does not necessarily increase the overall amount of click chemistry linkage. The concentrations used, along with the determined reaction time of 30 minutes, may already saturate the alkyne-azide linkages.

Our optimized labeling approach with saponified fatty acids and delipidated media has been shown to increase the detection of S-acylated proteins, which was most pronounced in fatty acids with more carbons, such as stearate, by improving their solubility. The data suggests that using delipidated media may further improve the incorporation of fatty acid analogs into cells. In addition, saponified fatty acids are likely to protect cells from lipotoxicity. By avoiding activation of unwanted pathways when adding fatty acids directly to cells, saponification may provide a different profile of S-acylated proteins, and thus be a more accurate representation of physiological cellular processes. This was observed in the alkyne-palmitate labeled proteins (Figure 3.4 and 3.5) with several bands showing

noticeably increased acylation signal in the saponified samples in delipidated media (Figure 3.4 and 3.5 middle panels). In such cases, even in the absence of a significant increase in overall acylation signal, which was also the case in alkyne myristate labeled cells, it is still beneficial to saponify fatty acids to protect cells from toxicity and maintain consistency when comparing the fatty acids analogs. On the other hand, 2BP did not inhibit palmitoylation whether it was added directly to cell culture or saponified. Interestingly, 2BP has been found to effect deacylation as well, therefore it may be difficult to distinguish whether 2BP is inhibiting acylation or increasing deacylation, resulting in no change in the total palmitoylation signal (Pedro et al., 2013). Future studies investigating saponification of 2BP would require a titration to determine the optimal concentration.

The majority of palmitoyl-proteome studies using metabolic labeling and click chemistry to date involved the use of 17-ODYA due to its commercial availability and relative low cost; 17-ODYA is also added directly to cells in regular media in these studies (Blanc et al., 2015). We have shown that 17-ODYA exhibited the most pronounced increase in fatty acylation signal detected by click chemistry when the fatty acids were saponified, incubated in FAFBSA, and added to delipidated media. Therefore, it is reasonable to speculate that some S-acylated proteins, especially low-abundance proteins, may have been missed due to decreased cellular availability of the alkynyl fatty acid label. In addition, there may be a change in the profile of protein S-acylation when fatty acids are added directly to media, which leads to toxicity and activation of cell death pathways (Listenberger et al., 2001; Wu et al., 2013; Yin et al., 2015). In addition, we demonstrated that protein acyltransferases have different preferences for palmitate and fatty acids with other hydrocarbon lengths, such as stearate (Jiang et al., 2018). This may introduce a bias in S-acylation detection favouring PATs that prefer stearate when labeled with 17-ODYA, undermining those that prefer palmitate.

Lastly, metabolic labeling with delipidated media and saponified fatty acids in FAFBSA was shown to improve the S-acylation signal in two different cell types, human HEK293T and mouse HT22 cells, suggesting that this improvement is likely applicable to a wide range of cells.

Chapter 4
Click Chemistry-Enabled Enrichment and Induction of Autophagy

The aim of this thesis project was to identify palmitoylated proteins during autophagy. Therefore, the enrichment of proteins following click chemistry linkage to an affinity probe would be critical in the study of fatty acylated proteins during autophagy. After optimization of fatty acid label delivery and click chemistry reagents, the next step was to optimize pulldown conditions for the enrichment of palmitoylated proteins. In addition, the conditions for autophagy induction also needed to be optimized in order to combine these techniques to induce autophagy simultaneously during metabolic labeling using detectable alkynyl fatty acid analogs. This will allow click chemistry-mediated linkage of an affinity probe for subsequent enrichment in order to facilitate the study of S-acylated proteins during autophagy and identify substrates with mass spectrometry.

The aim of the following set of experiments was to optimize the specific enrichment of S-acylated proteins following linkage of biotin through the click chemistry reaction between the azido and alkyne groups. In addition, chemical induction of autophagy during metabolic labeling was examined to enable click chemistry-based enrichment of S-acylated proteins during autophagy.

4.1 Biotin-based enrichment

Previously, click chemistry was used in the Martin lab for the detection of fatty acylated proteins only, where fluorescent azido probes were shown to be efficient and easy to visualize. For the purpose of affinity-based enrichment, however, biotin-based azido probes were necessary. To enable downstream purification, 5 to 10 times the typical amount of protein as previous detection experiments were reacted with corresponding volumes of click chemistry reagents according to the ratios stated in Chapter 2. This provided sufficient protein for affinity purification with avidin beads. The click chemistry reaction was stopped by precipitating the proteins with ice-cold acetone, instead

of denaturation in sample loading buffer. Two different methods of affinity enrichment were tested using either agarose neutravidin beads, or magnetic streptavidin beads.

In the first pulldown experiment, magnetic streptavidin beads were used following resuspension of the precipitated proteins in 0.1% SDS modified RIPA lysis buffer. Fatty acylated proteins were then released from the beads in 2X sample loading buffer with 4% β-mercaptoethanol by heating the samples at 95°C for 5 minutes, and then detected by western blotting. Preliminary results showed this method to be efficient in enriching S-acylated proteins labeled with alkynyl palmitate (Alk-pal) as well as N-myristoylated proteins labeled with alkynyl myristate (Figure 4.1 left). Importantly, proteins modified with unlabeled palmitate (without an alkyne group) showed minimal fatty acylation signal, suggesting that only a very small amount of background proteins not modified by the click chemistry-linked biotin were pulled down by the streptavidin beads (Figure 4.1 left). In addition, the signal in the palmitate labeled lanes also represent endogenously biotinylated proteins. However, the negligible amount of proteins in the palmitate labeled samples in comparison to the highly enriched fatty-acylated proteins in the alkyne labeled samples demonstrate the specificity of streptavidin pulldown following click chemistry. Since thioester bonds may sometimes be sensitive to β-mercaptoethanol (X. Wang et al., 2012), alkynyl myristate-modified proteins served as a control due to the resistance of amide bonds to reducing agents. However, there was no noticeable difference in fatty acylation signals between alkynyl myristate and alkynyl palmitate-modified proteins, suggesting that the usage of β-mercaptoethanol to release proteins from the streptavidin beads did not remove alkynyl palmitate from the eluted proteins (Figure 4.1).

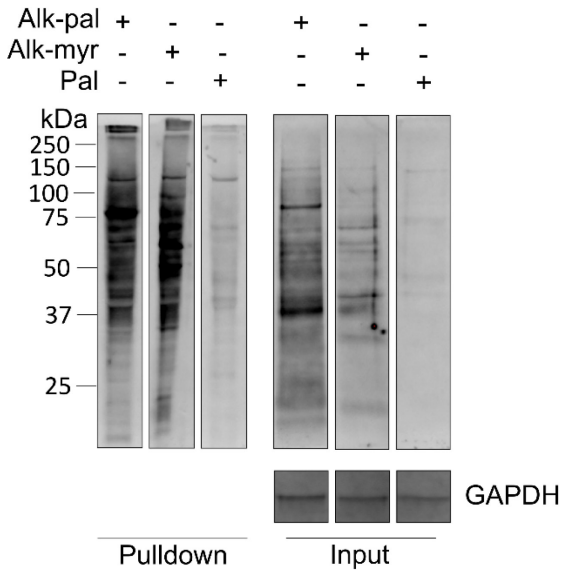

Figure 4.1 Total fatty acylation of streptavidin enriched S-acylated and N-myristoylated proteins following click chemistry.

HEK293T cells were labeled with the indicated fatty acids. 350 μg of protein were subjected to click chemistry linkage of Dde biotin azide plus to alkynyl fatty acid-modified proteins. Following acetone precipitation, fatty acylated proteins were pulled down with 30 uL of High Capacity Streptavidin Magnetic beads (Click Chemistry Tools) and released in 2X sample loading buffer (4% β-mercaptoethanol). Fatty acylation was detected with Alexa Fluor Streptavidin 680 Conjugate (Invitrogen). GAPDH was used as a loading control; anti-GAPDH rhodamine (1:5000).

The next experiment utilized a different approach to release biotinylated proteins from avidin beads, which was adapted from the acyl-biotin exchange (ABE) assay. The acyl-biotin exchange requires a similar enrichment step after endogenous palmitate is replaced with biotin. Therefore, we sought to compare the two different pulldown methods. Cells were transfected with the auto-palmitoylated protein acyltransferase zDHHC17 as a positive control (Jiang et al., 2018). The general palmitoylation inhibitor 2BP was also included and was expected to reduce the amount of alkynyl-palmitate-modified proteins that were pulled down. Following resuspension of acetone-precipitated proteins and pulldown with neutravidin beads, the proteins were washed with ABE dilution buffer with varying concentrations of NaCl. Release of proteins was facilitated via incubation for 10 minutes

at 37°C in dilution buffer containing 250 mM NaCl, 0.2% SDS and 1% β-mercaptoethanol. The proteins were then denatured in sample loading buffer for SDS-PAGE and western blotting detection. Preliminary results showed this method to be unsuccessful in enriching alkynyl fatty acid-modified proteins that were linked to biotin via click chemistry. The complete lack of signal in the pulldown for fatty acylation or zDHHC17 suggested that the pulldown samples contained no protein (Figure 4.2 left). Therefore, this method was unsuitable for use in the enrichment of palmitoylated proteins during autophagy.

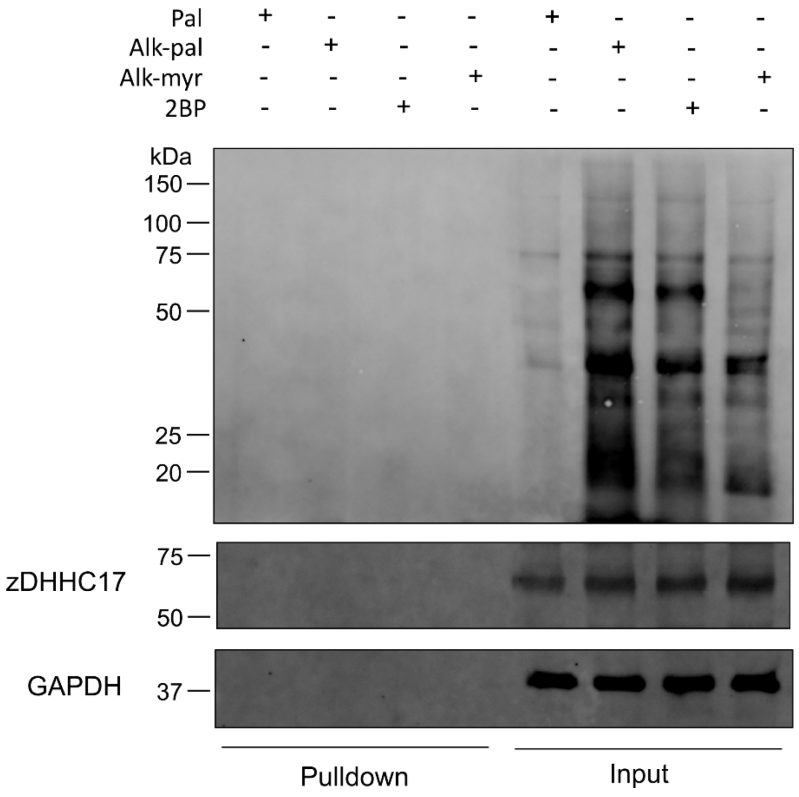

Figure 4.2 Total fatty acylation of neutravidin enriched S-acylated and N-myristoylated proteins following click chemistry.

HEK293T cells were transfected with zDHHC17-HA and labeled with the indicated fatty acids. 500 µg of protein were subjected to click chemistry linkage of Dde biotin azide plus to alkynyl fatty acid-modified proteins. Following acetone precipitation and resuspension in ABE lysis buffer, fatty acylated proteins were purified with 30 uL of High Capacity Neutravidin agarose beads (Thermo Scientific) and released following acyl-biotin exchange pulldown and elution protocol. Fatty acylation was detected with Alexa Fluor Streptavidin 680 Conjugate (Invitrogen). GAPDH was used as a loading control; anti-GAPDH rhodamine (1:5000).

4.2 Autophagy induction

After a viable method of biotin-based enrichment following click chemistry was established, we sought to incorporate chemical induction of autophagy into metabolic labeling with alkynyl fatty acid analogs. HeLa cells were used for autophagy experiments due to their well-characterized autophagic response (Muñoz-Braceras & Escalante, 2016; Taji et al., 2017). Rapamycin, a well-characterized

inducer of autophagy, acts directly on mTOR to initiate autophagy and is therefore used for chemical induction (Klionsky et al., 2021). Cells were treated for varying times ranging from 0 to 6 hours after labeling for 30 minutes with alkynyl palmitate or palmitate to determine the optimal length of the treatment period. Bafilomycin A1 was used to block fusion of the autophagosome to the lysosome to prevent the degradation of any palmitoylated proteins directed to the lysosome and to allow detection of p62 by preventing its degradation (Mauvezin & Neufeld, 2015). Preliminary results showed that treatment with rapamycin for 4 hours resulted in the most autophagic response with increased degradation of p62, as well as a noticeable increase in the conversion of LC3-I to LC3-II (Figure 4.3). Interestingly, while treatment for 2 hours yielded a considerably increased signal in total protein palmitoylation, it did not correspond with the same level of increase in autophagic flux measured by p62 degradation and LC3-I/II conversion as treatment for 4 hours or 6 hours, yet the amount of protein palmitoylation remained comparable between the three time points. This suggests that an upregulation of palmitoylation may need to occur upstream or within the early stages of autophagy, and that cells may need to maintain this increased level of palmitoylation to carry out autophagy in full.

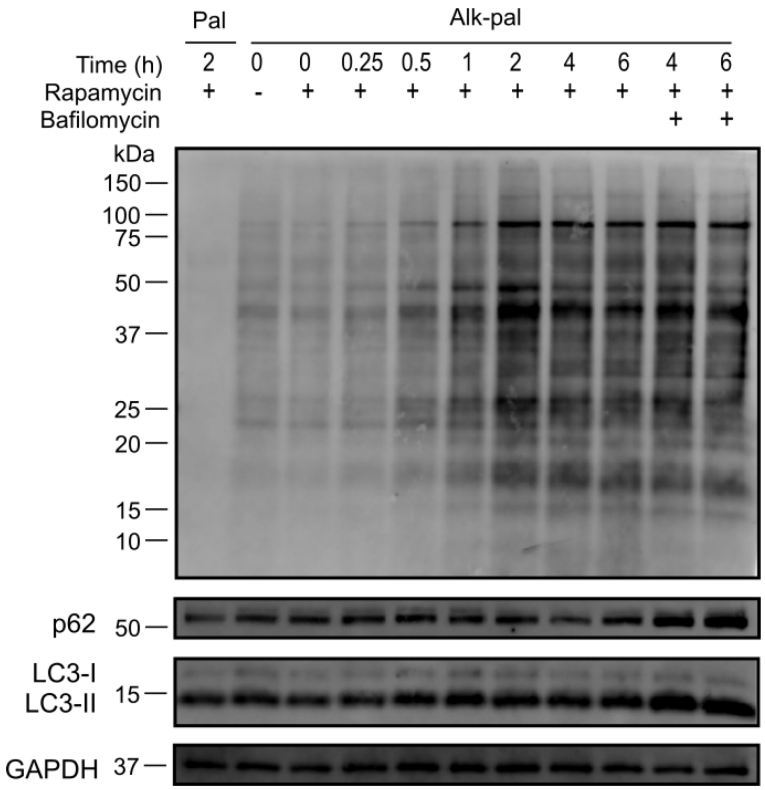

Figure 4.3 Total protein palmitoylation detection during rapamycin-induced autophagy.

HeLa cells were labeled with palmitic acid (Pal) and alkynyl palmitic acid (Alk-pal) for 30 minutes prior to the addition of 200 nM rapamycin or vehicle, with or without 100 nM bafilomycin A1 at the indicated times. Total protein lysates were subjected to click chemistry and alkynyl palmitate-modified proteins were detected using AFDye 647 azide plus (top panel). p62 (1:1000), and LC3I/II (1:1000) were probed separately. GAPDH was used as a loading control; anti-GAPDH rhodamine (1:5000).

From the rapamycin-induced autophagy experiments, we have determined that a treatment time of 4 hours yielded the most robust upregulation of autophagic flux. In combination with streptavidin pulldown following click chemistry linkage of biotin, and subsequent release in sample loading buffer with 4% β-mercaptoethanol, we can obtain highly enriched samples of proteins that undergo increased palmitoylation during autophagy for mass spectrometric identification.

4.3 Summary of results and discussion

I tested affinity purification of fatty acylated proteins linked to biotin through click chemistry. Pulldown using high capacity streptavidin beads were successful in enriching samples in fatty acylated proteins, with minimal detection of background biotinylated proteins. A second attempt using the ABE pulldown was unsuccessful and failed to obtain any protein in the pulldown. High capacity (HC) neutravidin and HC streptavidin beads have varying binding capacities. Magnetic beads are also more practical in comparison with agarose and better prevents the loss of beads during washes. Such considerations should be taken into account when selecting avidin beads for the pulldown of biotin-linked fatty acylated proteins.

It is also worth noting that while ABE also involves linking biotin to fatty acylated proteins, the mechanism of linkage and types of bonds are different. The ABE protocol used for pulldown shown in Figure 4.2 involves the use of HPDP-biotin which is a pyridyldithiol-biotin compound that forms reversible disulfide bonds with free cysteines (Soltec Ventures), while click chemistry-linked biotin azide occurs through a stable 1,2,3-triazole linkage (Devaraj et al., 2006). Therefore, HPDP-biotin linked proteins could be easily released in comparison to proteins linked to biotin through click chemistry. The use of Dde biotin azide plus allows for another option to release click chemistry-linked proteins with hydrazine, which should be tested if available. These pulldown experiments represented a preliminary trial of the two methods, and a more accurate comparison of the two pulldown methods in the future will require the use of consistent avidin beads between experiments side-by-side.

The increase in autophagic flux appeared to accompany an overall increase in total protein palmitoylation. However, an untreated control was lacking at each time point beyond 0 hours, therefore, whether palmitoylation was in fact upregulated remains to be confirmed. In particular,

levels of palmitoylation were noticeably elevated at 2 hours of rapamycin treatment and beyond, however, the increase in p62 degradation did not noticeably increase until 4 to 6 hours of treatment, although LC3-I/II conversation was slightly increased (Figure 4.3). Taken together, these results suggest that the increase in palmitoylation upon induction of autophagy may be more involved in the initial stages of autophagy, including formation of the double membraned autophagosome, when LC3-I/II conversion is essential (Tanida, 2011). In addition, the possible increase of total protein palmitoylation appeared to be prolonged throughout. This is consistent with a recent finding in the Martin lab that 50% of all autophagy regulators are palmitoylated (unpublished), therefore it is no surprise that palmitoylation levels remain elevated when autophagy is upregulated.

The experiment presented in Figure 4.3 aimed to identify the optimal treatment and labeling time for autophagy induction, which was found to be 4 hours. Next, a closer examination of these time points is required with an untreated control for each treatment period. In addition, it would be interesting to examine protein palmitoylation in closer detail as well by measuring changes in palmitoyl acyltransferases as well as protein thioesterases to determine whether the overall increase seen is due to increased forward palmitoylation, or a decrease in the reverse de-palmitoylation. Additionally, incorporation of a palmitoylation inhibitor would also provide further confirmation of whether palmitoylation affects autophagic flux.

In summary, this combined method has the potential to be a useful tool to examine the importance of protein palmitoylation in autophagy and provide insight on the mechanisms of diseases associated with disrupted autophagy.

Chapter 5

Low Throughput Confirmation and Characterization of Palmitoylated Proteins

The final objective of the project was to confirm and characterize proteins identified in the high throughput experiments. Since mass spectrometric analysis has yet to be completed, several proteins of interest to the Martin lab were analyzed for palmitoylation via metabolic labeling and click chemistry detection. The following experiments were performed for low throughput palmitoylation detection of the small valosin-containing protein (VCP) interacting protein (SVIP), and the SARS-CoV-2 spike protein (SARS-CoV-2 S). Through transfection with the proteins of interest prior to metabolic labeling, click chemistry can be performed on immunoprecipitated proteins as well as total protein lysates to confirm palmitoylation. Further characterization studies would also involve the acyl-biotin exchange assay in addition to click chemistry, as well as identifying sites of palmitoylation by mutating predicted cysteines.

5.1 Small VCP-interacting protein N-myristoylation and S-palmitoylation

Valosin-containing protein (VCP) is a highly conserved hexameric ATPase Associated with diverse cellular Activities (AAA) which include the ubiquitin-proteasome system in endoplasmic reticulum-associated protein degradation (ERAD), apoptosis, and autophagy (Yamanaka et al., 2012). VCP interacts with a large number of cofactors to allow its functioning in various compartments of the cell (Meyer & Weihl, 2014; Xia et al., 2016; Yeo & Yu, 2016). The 9-kDa small valosin containing protein/p97-interacting protein (SVIP) has been shown to regulate VCP localization (Nagahama et al., 2003; Y. Wang et al., 2011). In addition, overexpression of SVIP leads to the formation of vacuoles which colocalize with LC3 and the lysosomal marker lamp1, suggesting that the SVIP-VCP

interaction is involved in autophagy (Akcan et al., 2020; Y. Wang et al., 2011). Interestingly, potential myristoylation and palmitoylation sites have been identified at the N-terminus of SVIP, but not experimentally confirmed (Nagahama et al., 2003). This led to an interest to determine whether SVIP undergoes N-myristoylation and or S-palmitoylation, as well as the role these modifications may have on regulating SVIP function and its interaction with VCP. We therefore transfected mCherry-tagged SVIP (cloned in the Martin lab) into HEK293T cells and metabolically labeled with both alkynyl myristate and alkynyl palmitate, with or without the myristoylation inhibitor DDD85646 and the palmitoylation inhibitor 2BP. As a positive control, the known myristoylatable C-terminal truncated fragment of the huntingtin protein (myr-ctHTT-GFP) was included. A non-myristoylable form with a glycine to alanine substitiution (G2A-ctHTT-GFP) was also used (D. D. O. Martin et al., 2014). Both ctHTT-GFP plasmids were gifts from the Bertiaume lab.

To detect fatty acylation, the proteins were immunoprecipitated (IP) using the GFP or mCherry tags, then examined for fatty acylation through click chemistry. To ensure the assay was functional, total protein lysates were also clicked. As expected, myristoylation of myr-ctHTT-GFP was detected in both the lysates as well as immunoprecipitated proteins (Figure 5.1A top). Interestingly, the signal was stronger in the lysates in comparison to the IP, indicating efficient detection of fatty acylation without IP (Figure 5.1A top). In addition, the G2A mutation effectively abolished the detection of myristoylation in both lysates and immunoprecipitated G2A-ctHTT-GFP (Figure 5.1 bottom). Although the signal in the immunoprecipitated samples was noticeably weaker compared to the lysates, there was a substantial reduction in the presence of additional protein bands, suggesting increased specificity in the detection of a particular protein. The HTT results indicated that click chemistry detection on immunoprecipitated proteins following metabolic labeling with alkynyl fatty acid analogs was in fact, capable of detecting fatty acylation of an overexpressed protein while reducing background proteins present in the total protein lysate input (Figure 5.1A).

mCherry-tagged SVIP was detected at ~36 kDa in the lysates, and both myristoylation and palmitoylation were detected by click chemistry linkage of the alkynyl fatty acid-modified proteins in the SA680 channel (Figure 5.1B right). An additional band of ~12kDa in the lysates corresponding with endogenous SVIP, consistent with literature (Akcan et al., 2020; Nagahama et al., 2003), was also detected in the SA680 channel indicating that endogenous SVIP was myristoylated and palmitoylated (Figure 5.1B top right panel). However, mCherry-tagged SVIP was not detected in the IP. It was possible that the antibody used to IP mCherry-tagged SVIP was functional although weak, while the antibody used for western detection may have been ineffective. Nevertheless, although SVIP was not immunoprecipitated, we were able to detect SVIP fatty acylation in the lysates.

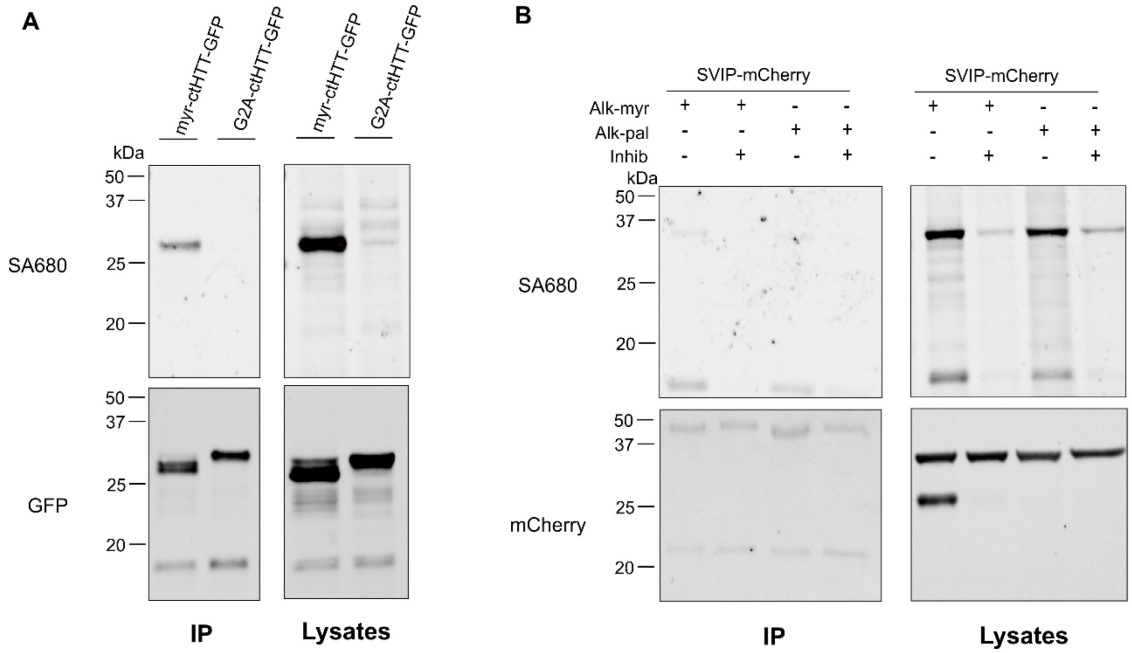

Figure 5.1 Fatty acylation detection of SVIP-mCherry and ctHTT-GFP via click chemistry.

HEK293T cells were transfected with SVIP-mCherry and ctHTT-GFP and metabolically labeled with alkynyl myristate or alkynyl palmitate in the presence or absence of inhibitors DDD85646 and 2BP where indicated. Following lysis, the proteins were immunoprecipitated and isolated using either anti-GFP or anti-mCherry antibodies and magnetic protein G beads. Both lysates and immunoprecipitated proteins released from beads were subjected to click chemistry. N-myristoylation and S-palmitoylation were detected using Alexa Fluor Streptavidin 680 Conjugate (SA680) (1:10,000). A) C-terminally truncated (ct) and myristoylatable form of huntingtin (HTT) (myr-ctHTT-GFP), and a non-myristoylatable form ctHTT-GFP with a G2A substitution (provided by the Bertiaume lab) were expressed. Goat anti-GFP was used for immunoprecipitation and detected using rabbit anti-GFP (1:5000) with anti-rabbit Alexa 488 (1:5000). B) mCherry-tagged SVIP (cloned in the Martin lab) was expressed. Mouse anti-mCherry was used for immunoprecipitation and mCherry was detected using mouse anti-mCherry (1:2500) with anti-mouse Alexa 555 (1:5000). Modified from**(Liao et al., 2021)**.

5.2 SARS-CoV-2 spike protein S-palmitoylation

In addition to SVIP, a second protein of interest was experimentally assessed specifically for palmitoylation. Recently, a large-scale interactome study of the severe acute respiratory syndrome coronavirus 2 (SARS-CoV-2) proteins, the cause of the current global pandemic, was completed in an effort to understand the molecular mechanisms of this virus (Gordon et al., 2020). Of the 26 proteins

that were expressed and purified for mass spectrometry identification, the spike protein of the virus (SARS-CoV-2 S) stood out due to its interaction with one of the mammalian protein acyltransferases (PAT), zDHHC5, suggesting that SARS-CoV-2 S may be S-acylated (Gordon et al., 2020). Covering the surface of the viral particles, the 180-200 kDa spike (S) protein has important functions in host cell entry through the mediation of receptor recognition and cell membrane fusion (Huang et al., 2020; F. Li, 2015). Since protein palmitoylation is known to facilitate membrane binding, in addition to the reported interaction with a PAT, strongly supported spike protein as a candidate for palmitoylation. Therefore, we sought to experimentally determine whether the spike protein is indeed modified by palmitoylation using metabolic labeling and click chemistry detection.

We obtained SARS-CoV-2 S from the interactome study and subsequently cloned it into FEW-mCherry (Dr. Dale Martin and Dr. Firyal Ramzan performed the cloning). mCherry-tagged SARS-CoV-2 S was transfected into HEK293T cells, with or without zDHHC5 or zDHHC20 and metabolically labeled with alkynyl palmitate. zDHHC20 was also included due to its similarities to zDHHC5 (Plain et al., 2020). Following lysis, immunoprecipitated proteins were subjected to click chemistry. We found several spike protein bands, especially at ~250 kDa, to be palmitoylated with the click chemistry-linked fluorescent azide signal (Figure 5.2), which indicated that the spike protein was acylated with alkynyl palmitate. The palmitoylation signal was largely abolished when the palmitoylation inhibitor 2BP was included during metabolic labeling, further confirming palmitoylation of the spike protein (Figure 5.2). Interestingly, co-transfection with zDHHC20 appeared to increase spike protein palmitoylation, whereas co-transfection with zDHHC5 seemed to change the banding pattern of the spike protein (Figure 5.2). Further studies in the Martin lab have since confirmed that both zDHHC5 and zDHHC20 increases Spike-mCherry palmitoylation and alters its cleavage patterns (unpublished). In addition, previous work by Dr. Martin and colleagues have identified ketoconazole as a novel palmitoylation inhibitor of the dual leucine-zipper kinase

(DLK), the palmitoylation of which is required for pro-degenerative signaling in axons (D. D. O. Martin et al., 2019). Since ketoconazole is an FDA-approved drug, we were curious to see if spike palmitoylation may be affected by ketoconazole as well. The palmitoylation signal seen in the larger fragment appears to be reduced with treatment of ketoconazole in comparison with the untreated sample (Figure 5.2), however, the mCherry signal was also reduced. Therefore, we cannot conclude whether ketoconazole had an inhibitory effect on palmitoylation of the spike protein of SARS-CoV-2.

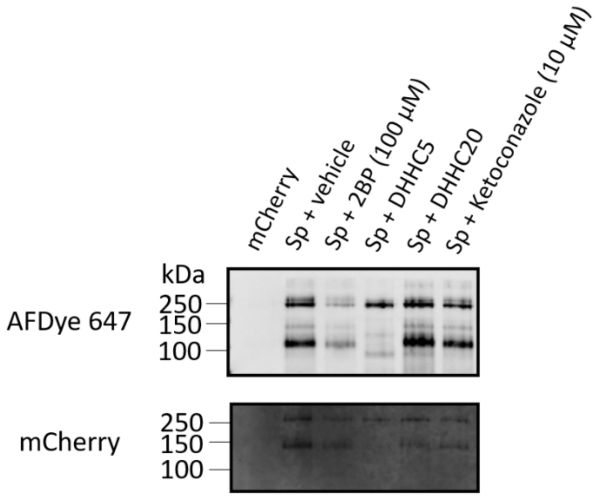

Figure 5.2 Palmitoylation detection of Spike-mCherry using click chemistry.

HEK293T cells were transfected with mCherry, mCherry-tagged SARS-CoV-2 S (Sp) and zDHHC5-HA or zDHHC20-HA as indicated. Cells were treated with 100 µM 2BP or 10 µM ketoconazole for 15 minutes where indicated, prior to metabolic labeling with alkynyl palmitate. Following lysis, spike-mCherry was immunoprecipitated and isolated using rabbit mCherry and magnetic protein G beads. Immunoprecipitated proteins released from the beads were subjected to click chemistry and palmitoylation was detected using AFDye 647 azide plus. mCherry was detected using rat anti-mCherry (1:2000) and anti-rat Alexa 488 (1:2500).

5.3 Summary of results and discussion

Through transfection and metabolic labeling in HEK293T cells with click chemistry detection, we have experimentally confirmed that SVIP is modified by both myristoylation and palmitoylation, while the spike protein of SARS-CoV-2 is modified by palmitoylation. Fatty acylation of SVIP has yet to be reported and has interesting implications on VCP function in autophagy, which further underlines the role of palmitoylation in autophagy. VCP functioning is largely dependent on its distribution within the cell, and recent work by Johnson and colleagues have shown that SVIP recruits VCP to the lysosome (Johnson et al., 2021). Interestingly, the study also found an inability for autophagosome fusion with lysosome using dual-tagged LC3 in SVIP knockout fruit flies, as well as an accumulation of insoluble protein aggregates (Johnson et al., 2021). These reported findings, in addition to our results confirming SVIP myristoylation and palmitoylation led to questions of whether the SVIP's interaction and recruitment of VCP to lysosomes are dependent on fatty acylation. The same research group has shown that the lysosome tubule network in muscles lose their stability and become fragmented, which disrupts autophagolysosome fusion, when VCP was mutated or SVIP knocked out (Johnson et al., 2015, 2021). It is possible that mutated SVIP incapable of fatty acylation would show the same effect of blocked autophagy. In addition, we found SVIP to be both myristoylated and palmitoylated, which was particularly interesting since dual acylation allows more complex regulation of membrane interactions (Farazi et al., 2001; D. D. O. Martin et al., 2011; Shahinian & Silvius, 1995). N-myristoylation promotes weak transient membrane interactions, while the reversibility of S-palmitoylation allows the dually-acylated protein to remain at the membrane until disengaged by the appropriate enzymes (Farazi et al., 2001; Shahinian & Silvius, 1995). Dual acylation of SVIP may therefore explain its importance in lysosome stability and late-stage autophagy involving fusion of the autophagosome with lysosomes. Ongoing studies in the Martin lab aim to test

the importance of SVIP fatty acylation on VCP localization and function, including the interplay between SVIP myristoylation and palmitoylation, especially under autophagic conditions.

Recently, the SARS-CoV-2 spike glycoproteins were found to be palmitoylated with the exchange-enabled mass tag labeling method which allows determination of the number of palmitoylated sites (Nguyen et al., 2020; Percher et al., 2016). Of the palmitoylated spike glycoproteins, different species showed one to four palmitoylated cysteines, which may explain our detection of multiple spike protein bands with at least one species modified by alkynyl palmitate (Figure 5.2) (Nguyen et al., 2020). The finding of SARS-CoV-2 spike protein palmitoylation may also present new target pathways for anti-viral therapeutics. 2BP-mediated inhibition of spike protein palmitoylation was found in a study by Nguyen and colleagues to reduce cleavage activation of the spike protein precursor, interfere with cellular fusion, and thereby reduce viral infection, suggesting a role of palmitoylation in proteolytic processing of the spike protein to facilitate cellular invasion (Nguyen et al., 2020). Consistent with the aforementioned study, another research group found pharmacological disruption of spike protein palmitoylation to prevent viral plaque formation and improve survival in mice infected with a murine CoV virus (M. Lee et al., 2020). In addition, both zDHHC5 and zDHHC20 were found to mediate spike protein palmitoylation, consistent with our findings, which functioned to regulate spike protein activation and cellular fusion (M. Lee et al., 2020; Mesquita et al., 2021). In light of the growing evidence implicating palmitoylation and spike protein-mediated infectivity of coronaviruses, targeting spike protein-specific palmitoylation may be a potentially promising therapeutic target.

Following experimental confirmation of fatty acylation in a protein of interest, the next steps to further characterize the effect of this modification will involve generating point mutations of predicted acylation sites. The Martin lab has generated cysteine and glycine point mutations in SVIP

to further understand the role of fatty acylation in the interaction and recruitment of VCP, as well as their roles in regulating the fate of autophagosomes during autophagy.

Chapter 6

Discussion

6.1 Conclusions and future directions

The aim of this research project was to optimize click chemistry-based methods of protein palmitoylation detection for the downstream identification of palmitoylated proteins that regulate autophagy. I have established functional protocols in the Martin lab for metabolic labeling and subsequent click chemistry detection by testing several reagents including fluorescent and biotin azides. Importantly, we have demonstrated that existing field practices of delivering fatty acid analogs were not as efficient as previously assumed and can be significantly improved upon by stripping cell culture media of fatty acids prior to the addition of saponified fatty acid analogs incubated in fatty acid-free BSA. This improved labeling approach has important implications for the study of protein palmitoylation due to the low sensitivity in the identification of palmitoylated proteins using the inefficient and insoluble fatty acid analog alkynyl stearate (17-ODYA) in palmitoylproteome studies, which likely led to the omission of a large number of palmitoylated protein targets (Liao et al., 2021). In addition, I have explored the combination of click chemistry detection with additional proteomic techniques, including affinity purification, to allow for focused analysis specifically on palmitoylated proteins within cells during chemically-induced autophagy. This enrichment is particularly important in our aim to identify new and high-value protein targets whose palmitoylation profile is dynamically regulated during autophagy.

There is considerable evidence supporting an interplay between protein palmitoylation, autophagy and neuronal functioning (Cho & Park, 2016; A. E.-D. El-Husseini & Bredt, 2002; Ji & Skup, 2021; Kim et al., 2018; Koster, 2019; Nakamura & Yoshimori, 2017; Sanders et al., 2015, 2019). Palmitoylation has been identified to be widely enriched in synaptic processes and disorders of the

central nervous system, which is not surprising due to the requirement of tightly regulated protein trafficking in the polarized morphologies of neurons (Fukata & Fukata, 2010; Sanders et al., 2015). In addition, a significant number of proteins associated with neurodegeneration have been identified to be palmitoylated. For example, disruptions in the peripheral postsynaptic density protein 95 (PSD-95) are associated with Alzheimer disease, and the targeting of PSD-95 to synaptic membranes is mediated by palmitoylation which then clusters ion channels (A. E. El-Husseini et al., 2000; Topinka & Bredt, 1998). Similarly, palmitoylation of many neuronal proteins including G-protein coupled receptors, signaling proteins such as Ras, neuronal cell adhesion molecules and synaptic vesicle proteins, like SNAP25, is important in regulating their function by mediating signaling, intracellular distribution, stability and anchorage in membrane interactions (Fukata & Fukata, 2010; Greaves & Chamberlain, 2011; Jia et al., 2014; Little et al., 2009). Therefore, protein palmitoylation is vital to neuronal functioning, and investigations into palmitoylation-mediated regulation of specific proteins can provide valuable insight into the mechanisms of pathology in diseases of the nervous system.

Remarkably, a number of proteins involved in autophagy that are also associated with neurodegeneration have been identified as palmitoylated in the Martin lab, which was a major motivation for this project. For example, presenilin 1 is required for lysosome acidification and proteolysis of substrates by cathepsins (J.-H. Lee et al., 2010) and was found to be palmitoylated (unpublished). Additionally, p62 palmitoylation was found to be decreased in Huntingtin (HD) diseased brains (unpublished), suggesting a role of p62 palmitoylation in the molecular mechanisms of HD. Similarly, valosin-containing protein (VCP) is involved in multiple stages of autophagy including initiation, maturation of the autophagosome, as well as fusion of the autophagolysosome (Yeo & Yu, 2016). Mutations of VCP cause diseases such as Inclusion body myopathy, Paget's bone disease, frontotemporal dementia, and amyotrophic lateral sclerosis (Vesa et al., 2009). Interestingly, we have found that both VCP, as well as the small VCP-interacting protein, are palmitoylated, which

leads us to speculate that this modification may contribute to their roles in late-stage autophagy in relation to the lysosome (unpublished) (Johnson et al., 2021). The possible overall increase in palmitoylation during rapamycin treatment would be in agreement with evidence supporting an enrichment of palmitoylation in autophagy in that 50% of all autophagy regulators are palmitoylated (unpublished). In combination with the successful enrichment following click chemistry linkage of biotin to palmitoylated proteins, future studies can proceed to identify palmitoylated proteins involved in autophagy by mass spectrometry with our collaborators at the University of Ottawa Dr. Mathieu Lavallee-Adam and Dr. Daniel Figeys. The combination of the improved metabolic labeling approach demonstrated in this project, along with the recently developed machine learning supervised real-time mass spectrometric identification developed by our collaborators, would further amplify sensitivity in the identification of palmitoylated protein targets (Pelletier et al., 2020). The resulting improvement in the detection of low abundance protein targets may identify novel substrates which undergo palmitoylation during autophagy.

Furthermore, we have demonstrated low throughput detection of two different proteins of interest via click chemistry of overexpressed proteins. This was performed on both immunoprecipitated proteins as well as total protein lysates to confirm palmitoylation and or myristoylation. Following identification of protein targets, the same low throughput confirmation of fatty acylation can be performed. In this regard, exchange-based methods should also be included to complement click chemistry-based detection to include stable protein palmitoylation with low turnover rates. Once confirmed, we can then aim to map sites of fatty acylation through site-directed mutagenesis of predicted sites and begin to characterize fatty acylation by determining the responsible protein acyltransferase(s) and examining changes in protein localization and cellular functions with immunofluorescence microscopy.

Autophagy is disrupted in a wide variety of diseases, whether due to an inability to clear toxic proteins and organelles, or through overactive degradation leading to autophagic cell death. Where impairment of autophagy is associated with disease, such as through the buildup of protein aggregates, we may expect to see a decrease in the overall levels of palmitoylation than normal within the cell. However, the profile of palmitoylated proteins in different types of diseases could be very different. For example, in cancer, palmitoylation regulates both pro-cancer oncogenes as well as tumour suppressors (Ko & Dixon, 2018). Ultimately, if we can determine how palmitoylation-regulated autophagy is disrupted in the pathogenesis of these diseases, it may provide potential targets to restore normal autophagic functions for the treatment of multiple disorders.

Letters of Copyright Permission

Liao, L. M. Q., Gray, R. A. V., & Martin, D. D. O. (2021). Optimized Incorporation of Alkynyl Fatty Acid Analogs for the Detection of Fatty Acylated Proteins using Click Chemistry. ***Journal of Visualized Experiments*****,** ***170*****. https://doi.org/10.3791/62107**

RE: JoVE Protocol 62107 Ready for Review Optimized Incorporation of Alkynyl Fatty Acid Analogs for the Detection of Fatty Acylated Proteins using Click Chemistry

"Hi Lucia,

Absolutely.

Please consider this explicit permission to reuse the JoVE content in your thesis. Please ensure that JoVE is cited properly throughout.

Thanks

Nam

--

Nam Nguyen, Ph.D.

Manager of Review

JoVE"

Jiang, H., Zhang, X., Chen, X., Aramsangtienchai, P., Tong, Z., & Lin, H. (2018). Protein Lipidation: Occurrence, Mechanisms, Biological Functions, and Enabling Technologies. *Chemical Reviews*, *118*(3), 919–988. https://doi.org/10.1021/acs.chemrev.6b00750

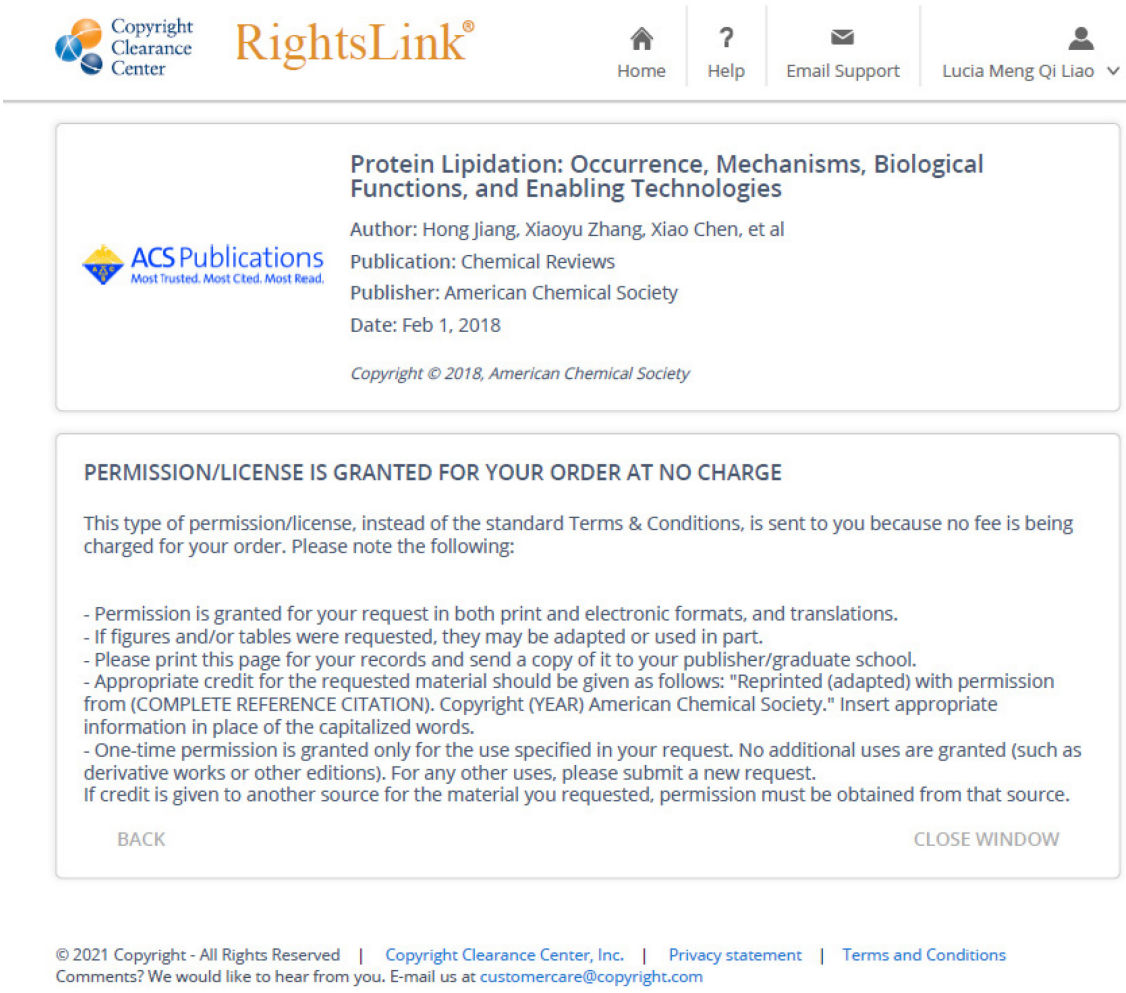

Martin, D. D. O., Ladha, S., Ehrnhoefer, D. E., & Hayden, M. R. (2015). Autophagy in Huntington disease and huntingtin in autophagy. *Trends in Neurosciences*, *38*(1), 26–35. https://doi.org/10.1016/j.tins.2014.09.003

Copyright Clearance Center RightsLink®

Home | Help | Email Support | Lucia Meng Qi Liao

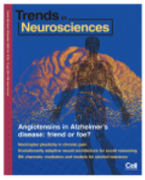

Autophagy in Huntington disease and huntingtin in autophagy

Author: Dale D.O. Martin,Saa ladha, Dagmar E Ehrnhoefer,Michael R Hayden
Publication: Trends in Neurosciences
Publisher: Elsevier
Date: January 2015

Order Completed

Thank you for your order.

This Agreement between Ms. Lucia Meng Qi Liao ("You") and Elsevier ("Elsevier") consists of your license details and the terms and conditions provided by Elsevier and Copyright Clearance Center.

Your confirmation email will contain your order number for future reference.

Printable Details

License Number	5051950671206
License date	Apr 18, 2021

Licensed Content

Licensed Content Publisher	Elsevier
Licensed Content Publication	Trends in Neurosciences
Licensed Content Title	Autophagy in Huntington disease and huntingtin in autophagy
Licensed Content Author	Dale D.O. Martin,Saa Ladha,Dagmar E. Ehrnhoefer,Michael R. Hayden
Licensed Content Date	Jan 1, 2015
Licensed Content Volume	38
Licensed Content Issue	1
Licensed Content Pages	10
Journal Type	S&T

Order Details

Type of Use	reuse in a thesis/dissertation
Portion	gures/tables/illustrations
Number of gures/tables/illustrations	1
Format	both print and electronic
Are you the author of this Elsevier article?	No
Will you be translating?	No

About Your Work

Title	Optimizing protein S-acylation detection in autophagy
Institution name	University of Waterloo
Expected presentation date	May 2021

Additional Data

Portions	Figure 1

Requestor Location

Ms. Lucia Meng Qi Liao
179 Napoli Court

Requestor Location

Hamilton, ON L9C 7A2
Canada
Attn: Ms. Lucia Meng Qi Liao

Price

Total 0.00 CAD

Tax Details

Publisher Tax ID GB 494 6272 12

Total: 0.00 CAD

CLOSE WINDOW ORDER MORE

References

Akcan, G., Alimogullari, E., Abu-Issa, R., & Cayli, S. (2020). Analysis of the developmental expression of small VCP-interacting protein and its interaction with steroidogenic acute regulatory protein in Leydig cells. *Reproductive Biology*, *20*(1), 88–96. https://doi.org/10.1016/j.repbio.2020.01.006

Al-Bari, Md. A. A. (2020). A current view of molecular dissection in autophagy machinery. *Journal of Physiology and Biochemistry*, *76*(3), 357–372. https://doi.org/10.1007/s13105-020-00746-0

Alsabeeh, N., Chausse, B., Kakimoto, P. A., Kowaltowski, A. J., & Shirihai, O. (2018). Cell culture models of fatty acid overload: Problems and solutions. *Biochimica et Biophysica Acta (BBA) - Molecular and Cell Biology of Lipids*, *1863*(2), 143–151. https://doi.org/10.1016/j.bbalip.2017.11.006

Blanc, M., David, F., Abrami, L., Migliozzi, D., Armand, F., Bürgi, J., & van der Goot, F. G. (2015). SwissPalm: Protein Palmitoylation database. *F1000Research*, *4*, 261. https://doi.org/10.12688/f1000research.6464.1

Braun, P. E., & Radin, N. S. (1969). Interactions of lipids with a membrane structural protein from myelin. *Biochemistry*, *8*(11), 4310–4318. https://doi.org/10.1021/bi00839a014

Chamberlain, L. H., & Shipston, M. J. (2015). The physiology of protein S-acylation. *Physiological Reviews*, *95*(2), 341–376. https://doi.org/10.1152/physrev.00032.2014

Cho, E., & Park, M. (2016). Palmitoylation in Alzheimer's disease and other neurodegenerative diseases. *Pharmacological Research*, *111*, 133–151. https://doi.org/10.1016/j.phrs.2016.06.008

Condello, M., Pellegrini, E., Caraglia, M., & Meschini, S. (2019). Targeting Autophagy to Overcome Human Diseases. *International Journal of Molecular Sciences*, *20*(3), 725. https://doi.org/10.3390/ijms20030725

Devaraj, N. K., Decreau, R. A., Ebina, W., Collman, J. P., & Chidsey, C. E. D. (2006). Rate of Interfacial Electron Transfer through the 1,2,3-Triazole Linkage. *The Journal of Physical Chemistry B*, *110*(32), 15955–15962. https://doi.org/10.1021/jp057416p

Drisdel, R. C., Alexander, J. K., Sayeed, A., & Green, W. N. (2006). Assays of protein palmitoylation. *Methods*, *40*(2), 127–134. https://doi.org/10.1016/j.ymeth.2006.04.015

El-Husseini, A. E., Craven, S. E., Chetkovich, D. M., Firestein, B. L., Schnell, E., Aoki, C., & Bredt, D. S. (2000). Dual Palmitoylation of Psd-95 Mediates Its Vesiculotubular Sorting, Postsynaptic Targeting, and Ion Channel Clustering. *The Journal of Cell Biology*, *148*(1), 159–172. https://doi.org/10.1083/jcb.148.1.159

El-Husseini, A. E.-D., & Bredt, D. S. (2002). Protein palmitoylation: a regulator of neuronal development and function. *Nature Reviews Neuroscience*, *3*(10), 791–802. https://doi.org/10.1038/nrn940

Farazi, T. A., Waksman, G., & Gordon, J. I. (2001). The Biology and Enzymology of ProteinN-Myristoylation* 210. *Journal of Biological Chemistry*, *276*(43), 39501–39504. https://doi.org/10.1074/jbc.r100042200

Fukata, Y., & Fukata, M. (2010). Protein palmitoylation in neuronal development and synaptic plasticity. *Nature Reviews Neuroscience*, *11*(3), 161–175. https://doi.org/10.1038/nrn2788

Gao, X., & Hannoush, R. N. (2017). A Decade of Click Chemistry in Protein Palmitoylation: Impact on Discovery and New Biology. *Cell Chemical Biology*, *ACS Chem. Biol. 1 2006*. https://doi.org/10.1016/j.chembiol.2017.12.002

Gordon, D. E., Jang, G. M., Bouhaddou, M., Xu, J., Obernier, K., White, K. M., O'Meara, M. J., Rezelj, V. V., Guo, J. Z., Swaney, D. L., Tummino, T. A., Hüttenhain, R., Kaake, R. M., Richards, A. L., Tutuncuoglu, B., Foussard, H., Batra, J., Haas, K., Modak, M., … Krogan, N. J. (2020). A SARS-CoV-2 protein interaction map reveals targets for drug repurposing. *Nature*, *583*(7816), 459–468. https://doi.org/10.1038/s41586-020-2286-9

Greaves, J., & Chamberlain, L. H. (2011). Differential palmitoylation regulates intracellular patterning of SNAP25. *Journal of Cell Science*, *124*(8), 1351–1360. https://doi.org/10.1242/jcs.079095

Hang, H. C., Geutjes, E.-J., Grotenbreg, G., Pollington, A. M., Bijlmakers, M. J., & Ploegh, H. L. (2007). Chemical Probes for the Rapid Detection of Fatty-Acylated Proteins in Mammalian Cells. *Journal of the American Chemical Society*, *129*(10), 2744–2745. https://doi.org/10.1021/ja0685001

Hang, H. C., Wilson, J. P., & Charron, G. (2011). Bioorthogonal Chemical Reporters for Analyzing Protein Lipidation and Lipid Trafficking. *Accounts of Chemical Research*, *44*(9), 699–708. https://doi.org/10.1021/ar200063v

Hang, H. C., Yu, C., Kato, D. L., & Bertozzi, C. R. (2003). A metabolic labeling approach toward proteomic analysis of mucin-type O-linked glycosylation. *Proceedings of the National Academy of Sciences*, *100*(25), 14846–14851. https://doi.org/10.1073/pnas.2335201100

Heal, W. P., Wickramasinghe, S. R., Bowyer, P. W., Holder, A. A., Smith, D. F., Leatherbarrow, R. J., & Tate, E. W. (2007). Site-specific N-terminal labelling of proteins in vitro and in vivo using N-myristoyl transferase and bioorthogonal ligation chemistry. *Chemical Communications*, *0*(4), 480–482. https://doi.org/10.1039/b716115h

Heal, W. P., Wickramasinghe, S. R., Leatherbarrow, R. J., & Tate, E. W. (2008). N -Myristoyl transferase-mediated protein labelling in vivo. *Organic & Biomolecular Chemistry*, *6*(13), 2308–2315. https://doi.org/10.1039/b803258k

Holland, S. M., Collura, K. M., Ketschek, A., Noma, K., Ferguson, T. A., Jin, Y., Gallo, G., & Thomas, G. M. (2016). Palmitoylation controls DLK localization, interactions and activity to ensure effective axonal injury signaling. *Proceedings of the National Academy of Sciences*, *113*(3), 763–768. https://doi.org/10.1073/pnas.1514123113

Hong, V., Steinmetz, N. F., Manchester, M., & Finn, M. G. (2010). Labeling Live Cells by Copper-Catalyzed Alkyne−Azide Click Chemistry. *Bioconjugate Chemistry*, *21*(10), 1912–1916. https://doi.org/10.1021/bc100272z

Huang, Y., Yang, C., Xu, X., Xu, W., & Liu, S. (2020). Structural and functional properties of SARS-CoV-2 spike protein: potential antivirus drug development for COVID-19. *Acta Pharmacologica Sinica*, *41*(9), 1141–1149. https://doi.org/10.1038/s41401-020-0485-4

Ji, B., & Skup, M. (2021). Roles of palmitoylation in structural long-term synaptic plasticity. *Molecular Brain*, *14*(1), 8. https://doi.org/10.1186/s13041-020-00717-y

Jia, L., Chisari, M., Maktabi, M. H., Sobieski, C., Zhou, H., Konopko, A. M., Martin, B. R., Mennerick, S. J., & Blumer, K. J. (2014). A Mechanism Regulating G Protein-coupled Receptor Signaling That Requires Cycles of Protein Palmitoylation and Depalmitoylation* ♦. *Journal of Biological Chemistry*, *289*(9), 6249–6257. https://doi.org/10.1074/jbc.m113.531475

Jiang, H., Zhang, X., Chen, X., Aramsangtienchai, P., Tong, Z., & Lin, H. (2018). Protein Lipidation: Occurrence, Mechanisms, Biological Functions, and Enabling Technologies. *Chemical Reviews*, *118*(3), 919–988. https://doi.org/10.1021/acs.chemrev.6b00750

Johnson, A. E., Orr, B. O., Fetter, R. D., Moughamian, A. J., Primeaux, L. A., Geier, E. G., Yokoyama, J. S., Miller, B. L., & Davis, G. W. (2021). SVIP is a molecular determinant of lysosomal dynamic stability, neurodegeneration and lifespan. *Nature Communications*, *12*(1), 513. https://doi.org/10.1038/s41467-020-20796-8

Johnson, A. E., Shu, H., Hauswirth, A. G., Tong, A., & Davis, G. W. (2015). VCP-dependent muscle degeneration is linked to defects in a dynamic tubular lysosomal network in vivo. *ELife*, *4*, e07366. https://doi.org/10.7554/elife.07366

Jordan, M., Schallhorn, A., & Wurm, F. M. (1996). Transfecting Mammalian Cells: Optimization of Critical Parameters Affecting Calcium-Phosphate Precipitate Formation. *Nucleic Acids Research*, *24*(4), 596–601. https://doi.org/10.1093/nar/24.4.596

Keller, C. A., Yuan, X., Panzanelli, P., Martin, M. L., Alldred, M., Sassoè-Pognetto, M., & Lüscher, B. (2004). The γ2 Subunit of GABAA Receptors Is a Substrate for Palmitoylation by GODZ. *The Journal of Neuroscience*, *24*(26), 5881–5891. https://doi.org/10.1523/jneurosci.1037-04.2004

Khan, M. M., Strack, S., Wild, F., Hanashima, A., Gasch, A., Brohm, K., Reischl, M., Carnio, S., Labeit, D., Sandri, M., Labeit, S., & Rudolf, R. (2013). Role of autophagy, SQSTM1, SH3GLB1, and TRIM63 in the turnover of nicotinic acetylcholine receptors. *Autophagy*, *10*(1), 123–136. https://doi.org/10.4161/auto.26841

Khoury, G. A., Baliban, R. C., & Floudas, C. A. (2011). Proteome-wide post-translational modification statistics: frequency analysis and curation of the swiss-prot database. *Scientific Reports*, *1*(1), 90. https://doi.org/10.1038/srep00090

Kim, S. W., Kim, D. H., Park, K. S., Kim, M. K., Park, Y. M., Muallem, S., So, I., & Kim, H. J. (2018). Palmitoylation controls trafficking of the intracellular Ca2+ channel MCOLN3/TRPML3 to regulate autophagy. *Autophagy*, *15*(2), 327–340. https://doi.org/10.1080/15548627.2018.1518671

Kit, M. C. S., & Martin, B. R. (2019). Protein Lipidation, Methods and Protocols. *Methods in Molecular Biology (Clifton, N.J.)*, *2009*, 71–79. https://doi.org/10.1007/978-1-4939-9532-5_6

Klionsky, D. J., Abdel-Aziz, A. K., Abdelfatah, S., Abdellatif, M., Abdoli, A., Abel, S., Abeliovich, H., Abildgaard, M. H., Abudu, Y. P., Acevedo-Arozena, A., Adamopoulos, I. E., Adeli, K., Adolph, T. E., Adornetto, A., Aflaki, E., Agam, G., Agarwal, A., Aggarwal, B. B., Agnello, M., … Tong, C.-K. (2021). Guidelines for the use and interpretation of assays for monitoring autophagy (4th edition). *Autophagy*, 1–382. https://doi.org/10.1080/15548627.2020.1797280

Ko, P., & Dixon, S. J. (2018). Protein palmitoylation and cancer. *EMBO Reports*, *19*(10). https://doi.org/10.15252/embr.201846666

Koster, K. P. (2019). AMPAR Palmitoylation Tunes Synaptic Strength: Implications for Synaptic Plasticity and Disease. *Journal of Neuroscience*, *39*(26), 5040–5043. https://doi.org/10.1523/jneurosci.0055-19.2019

Kostiuk, M. A., Corvi, M. M., Keller, B. O., Plummer, G., Prescher, J. A., Hangauer, M. J., Bertozzi, C. R., Rajaiah, G., Falck, J. R., & Berthiaume, L. G. (2008). Identification of palmitoylated mitochondrial proteins using a bio-orthogonal azido-palmitate analogue. *The FASEB Journal*, *22*(3), 721–732. https://doi.org/10.1096/fj.07-9199com

Lee, J.-H., Yu, W. H., Kumar, A., Lee, S., Mohan, P. S., Peterhoff, C. M., Wolfe, D. M., Martinez-Vicente, M., Massey, A. C., Sovak, G., Uchiyama, Y., Westaway, D., Cuervo, A. M., & Nixon, R. A. (2010). Lysosomal Proteolysis and Autophagy Require Presenilin 1 and Are Disrupted by Alzheimer-Related PS1 Mutations. *Cell*, *141*(7), 1146–1158. https://doi.org/10.1016/j.cell.2010.05.008

Lee, M., Sugiyama, M., Mekhail, K., Latreille, E., Khosraviani, N., Wei, K., Lee, W. L., Antonescu, C., & Fairn, G. D. (2020). Fatty Acid Synthase inhibition prevents palmitoylation of SARS-CoV2 Spike Protein and improves survival of mice infected with murine hepatitis virus. *BioRxiv*, 2020.12.20.423603. https://doi.org/10.1101/2020.12.20.423603

Lemonidis, K., Salaun, C., Kouskou, M., Diez-Ardanuy, C., Chamberlain, L. H., & Greaves, J. (2017). Substrate selectivity in the zDHHC family of S -acyltransferases. *Biochemical Society Transactions*, *45*(3), 751–758. https://doi.org/10.1042/bst20160309

Lemonidis, K., Sanchez-Perez, M. C., & Chamberlain, L. H. (2015). Identification of a Novel Sequence Motif Recognized by the Ankyrin Repeat Domain of zDHHC17/13 S-Acyltransferases. *Journal of Biological Chemistry*, *290*(36), 21939–21950. https://doi.org/10.1074/jbc.m115.657668

Levine, B., & Kroemer, G. (2008). Autophagy in the Pathogenesis of Disease. *Cell*, *132*(1), 27–42. https://doi.org/10.1016/j.cell.2007.12.018

Li, F. (2015). Structure, Function, and Evolution of Coronavirus Spike Proteins. *Annual Review of Virology*, *3*(1), 1–25. https://doi.org/10.1146/annurev-virology-110615-042301

Li, Z., Berk, M., McIntyre, T. M., Gores, G. J., & Feldstein, A. E. (2008). The lysosomal-mitochondrial axis in free fatty acid–induced hepatic lipotoxicity. *Hepatology*, *47*(5), 1495–1503. https://doi.org/10.1002/hep.22183

Liao, L. M. Q., Gray, R. A. V., & Martin, D. D. O. (2021). Optimized Incorporation of Alkynyl Fatty Acid Analogs for the Detection of Fatty Acylated Proteins using Click Chemistry. *Journal of Visualized Experiments*, *170*. https://doi.org/10.3791/62107

Lin, D. T. S., & Conibear, E. (2015). ABHD17 proteins are novel protein depalmitoylases that regulate N-Ras palmitate turnover and subcellular localization. *ELife*, *4*, e11306. https://doi.org/10.7554/elife.11306

Linder, M. E., & Deschenes, R. J. (2007). Palmitoylation: policing protein stability and traffic. *Nature Reviews Molecular Cell Biology*, *8*(1), 74–84. https://doi.org/10.1038/nrm2084

Listenberger, L. L., Ory, D. S., & Schaffer, J. E. (2001). Palmitate-induced Apoptosis Can Occur through a Ceramide-independent Pathway*. *Journal of Biological Chemistry*, *276*(18), 14890–14895. https://doi.org/10.1074/jbc.m010286200

Little, E. B., Edelman, G. M., & Cunningham, B. A. (2009). Palmitoylation of the Cytoplasmic Domain of the Neural Cell Adhesion Molecule N-CAM Serves as an Anchor to Cellular Membranes. *Cell Communication & Adhesion*, *6*(5), 415–430. https://doi.org/10.3109/15419069809109150

Lobo, S., Greentree, W. K., Linder, M. E., & Deschenes, R. J. (2002). Identification of a Ras Palmitoyltransferase inSaccharomyces cerevisiae *. *Journal of Biological Chemistry*, *277*(43), 41268–41273. https://doi.org/10.1074/jbc.m206573200

Long, J. Z., & Cravatt, B. F. (2011). The Metabolic Serine Hydrolases and Their Functions in Mammalian Physiology and Disease. *Chemical Reviews*, *111*(10), 6022–6063. https://doi.org/10.1021/cr200075y

Majmudar, J. D., & Martin, B. R. (2014). Strategies for profiling native S-nitrosylation. *Biopolymers*, *101*(2), 173–179. https://doi.org/10.1002/bip.22342

Martin, B. R., & Cravatt, B. F. (2009). Large-scale profiling of protein palmitoylation in mammalian cells. *Nature Methods*, *6*(2), 135–138. https://doi.org/10.1038/nmeth.1293

Martin, B. R., Wang, C., Adibekian, A., Tully, S. E., & Cravatt, B. F. (2012). Global profiling of dynamic protein palmitoylation. *Nature Methods*, *9*(1), 84–89. https://doi.org/10.1038/nmeth.1769

Martin, D. D. O., Beauchamp, E., & Berthiaume, L. G. (2011). Post-translational myristoylation: Fat matters in cellular life and death. *Biochimie*, *93*(1), 18–31. https://doi.org/10.1016/j.biochi.2010.10.018

Martin, D. D. O., Heit, R. J., Yap, M. C., Davidson, M. W., Hayden, M. R., & Berthiaume, L. G. (2014). Identification of a post-translationally myristoylated autophagy-inducing domain released by caspase cleavage of Huntingtin. *Human Molecular Genetics*, *23*(12), 3166–3179. https://doi.org/10.1093/hmg/ddu027

Martin, D. D. O., Kanuparthi, P. S., Holland, S. M., Sanders, S. S., Jeong, H.-K., Einarson, M. B., Jacobson, M. A., & Thomas, G. M. (2019). Identification of Novel Inhibitors of DLK Palmitoylation and Signaling by High Content Screening. *Scientific Reports*, *9*(1), 3632. https://doi.org/10.1038/s41598-019-39968-8

Martin, D. D. O., Ladha, S., Ehrnhoefer, D. E., & Hayden, M. R. (2015). Autophagy in Huntington disease and huntingtin in autophagy. *Trends in Neurosciences*, *38*(1), 26–35. https://doi.org/10.1016/j.tins.2014.09.003

Martin, D. D. O., Vilas, G. L., Prescher, J. A., Rajaiah, G., Falck, J. R., Bertozzi, C. R., & Berthiaume, L. G. (2008). Rapid detection, discovery, and identification of post-translationally myristoylated proteins during apoptosis using a bio-orthogonal azidomyristate analog. *The FASEB Journal*, *22*(3), 797–806. https://doi.org/10.1096/fj.07-9198com

Mauvezin, C., & Neufeld, T. P. (2015). Bafilomycin A1 disrupts autophagic flux by inhibiting both V-ATPase-dependent acidification and Ca-P60A/SERCA-dependent autophagosome-lysosome fusion. *Autophagy*, *11*(8), 1437–1438. https://doi.org/10.1080/15548627.2015.1066957

Menzies, F. M., Fleming, A., Caricasole, A., Bento, C. F., Andrews, S. P., Ashkenazi, A., Füllgrabe, J., Jackson, A., Sanchez, M. J., Karabiyik, C., Licitra, F., Ramirez, A. L., Pavel, M., Puri, C., Renna, M., Ricketts, T., Schlotawa, L., Vicinanza, M., Won, H., … Rubinsztein, D. C. (2017). Autophagy and Neurodegeneration: Pathogenic Mechanisms and Therapeutic Opportunities. *Neuron*, *93*(5), 1015–1034. https://doi.org/10.1016/j.neuron.2017.01.022

Mesquita, F. S., Abrami, L., Sergeeva, O., Turelli, P., Kunz, B., Raclot, C., Montoya, J. P., Abriata, L. A., Peraro, M. D., Trono, D., D'Angelo, G., & van der Goot, F. G. (2021). S-acylation controls SARS-Cov-2 membrane lipid organization and enhances infectivity. *BioRxiv*, 2021.03.14.435299. https://doi.org/10.1101/2021.03.14.435299

Meyer, H., & Weihl, C. C. (2014). The VCP/p97 system at a glance: connecting cellular function to disease pathogenesis. *Journal of Cell Science*, *127*(18), 3877–3883. https://doi.org/10.1242/jcs.093831

Muñoz-Braceras, S., & Escalante, R. (2016). Analysis of Relevant Parameters for Autophagic Flux Using HeLa Cells Expressing EGFP-LC3. *Methods in Molecular Biology*, *1449*, 313–329. https://doi.org/10.1007/978-1-4939-3756-1_20

Nagahama, M., Suzuki, M., Hamada, Y., Hatsuzawa, K., Tani, K., Yamamoto, A., & Tagaya, M. (2003). SVIP Is a Novel VCP/p97-interacting Protein Whose Expression Causes Cell Vacuolation. *Molecular Biology of the Cell*, *14*(1), 262–273. https://doi.org/10.1091/mbc.02-07-0115

Nakamura, S., & Yoshimori, T. (2017). New insights into autophagosome–lysosome fusion. *J Cell Sci*, *130*(7), jcs.196352. https://doi.org/10.1242/jcs.196352

Nguyen, H. T., Zhang, S., Wang, Q., Anang, S., Wang, J., Ding, H., Kappes, J. C., & Sodroski, J. (2020). Spike Glycoprotein and Host Cell Determinants of SARS-CoV-2 Entry and Cytopathic Effects. *Journal of Virology*, *95*(5). https://doi.org/10.1128/jvi.02304-20

Ohno, Y., Kihara, A., Sano, T., & Igarashi, Y. (2006). Intracellular localization and tissue-specific distribution of human and yeast DHHC cysteine-rich domain-containing proteins. *Biochimica et Biophysica Acta (BBA) - Molecular and Cell Biology of Lipids*, *1761*(4), 474–483. https://doi.org/10.1016/j.bbalip.2006.03.010

Parzych, K. R., & Klionsky, D. J. (2013). An overview of autophagy: morphology, mechanism, and regulation. *Antioxidants & Redox Signaling*, *20*(3), 460–473. https://doi.org/10.1089/ars.2013.5371

Pedro, M. P., Vilcaes, A. A., Tomatis, V. M., Oliveira, R. G., Gomez, G. A., & Daniotti, J. L. (2013). 2-Bromopalmitate Reduces Protein Deacylation by Inhibition of Acyl-Protein Thioesterase Enzymatic Activities. *PLoS ONE*, *8*(10), e75232. https://doi.org/10.1371/journal.pone.0075232

Pelletier, A. R., Chung, Y.-E., Ning, Z., Wong, N., Figeys, D., & Lavallée-Adam, M. (2020). MealTime-MS: A Machine Learning-Guided Real-Time Mass Spectrometry Analysis for Protein Identification and Efficient Dynamic Exclusion. *BioRxiv*, 2020.05.22.110726. https://doi.org/10.1101/2020.05.22.110726

Percher, A., Ramakrishnan, S., Thinon, E., Yuan, X., Yount, J. S., & Hang, H. C. (2016). Mass-tag labeling reveals site-specific and endogenous levels of protein S-fatty acylation. *Proceedings of the National Academy of Sciences*, *113*(16), 4302–4307. https://doi.org/10.1073/pnas.1602244113

Plain, F., Howie, J., Kennedy, J., Brown, E., Shattock, M. J., Fraser, N. J., & Fuller, W. (2020). Control of protein palmitoylation by regulating substrate recruitment to a zDHHC-protein acyltransferase. *Communications Biology*, *3*(1), 411. https://doi.org/10.1038/s42003-020-01145-3

Presolski, S. I., Hong, V. P., & Finn, M. G. (2011). Copper-Catalyzed Azide–Alkyne Click Chemistry for Bioconjugation. *Current Protocols in Chemical Biology*, *3*(4), 153–162. https://doi.org/10.1002/9780470559277.ch110148

Ra, E. A., Lee, T. A., Kim, S. W., Park, A., Choi, H. jin, Jang, I., Kang, S., Cheon, J. H., Cho, J. W., Lee, J. E., Lee, S., & Park, B. (2016). TRIM31 promotes Atg5/Atg7-independent autophagy in intestinal cells. *Nature Communications*, *7*(1), 11726. https://doi.org/10.1038/ncomms11726

Rana, M. S., Kumar, P., Lee, C.-J., Verardi, R., Rajashankar, K. R., & Banerjee, A. (2018). Fatty acyl recognition and transfer by an integral membrane S -acyltransferase. *Science*, *359*(6372), eaao6326. https://doi.org/10.1126/science.aao6326

Reddy, K. D., Malipeddi, J., DeForte, S., Pejaver, V., Radivojac, P., Uversky, V. N., & Deschenes, R. J. (2016). Physicochemical sequence characteristics that influence S-palmitoylation propensity. *Journal of Biomolecular Structure and Dynamics*, *35*(11), 1–14. https://doi.org/10.1080/07391102.2016.1217275

Resh, M. D. (2016). Fatty acylation of proteins: The long and the short of it. *Progress in Lipid Research*, *63*, 120–131. https://doi.org/10.1016/j.plipres.2016.05.002

Roth, A. F., Feng, Y., Chen, L., & Davis, N. G. (2002). The yeast DHHC cysteine-rich domain protein Akr1p is a palmitoyl transferase. *The Journal of Cell Biology*, *159*(1), 23–28. https://doi.org/10.1083/jcb.200206120

Roth, A. F., Wan, J., Bailey, A. O., Sun, B., Kuchar, J. A., Green, W. N., Phinney, B. S., Yates, J. R., & Davis, N. G. (2006). Global Analysis of Protein Palmitoylation in Yeast. *Cell*, *125*(5), 1003–1013. https://doi.org/10.1016/j.cell.2006.03.042

Sanders, S. S., Martin, D. D. O., Butland, S. L., Lavallée-Adam, M., Calzolari, D., Kay, C., Yates, J. R., & Hayden, M. R. (2015). Curation of the Mammalian Palmitoylome Indicates a Pivotal Role for Palmitoylation in Diseases and Disorders of the Nervous System and Cancers. *PLOS Computational Biology*, *11*(8), e1004405. https://doi.org/10.1371/journal.pcbi.1004405

Sanders, S. S., Simone, F. I. D., & Thomas, G. M. (2019). mTORC1 Signaling Is Palmitoylation-Dependent in Hippocampal Neurons and Non-neuronal Cells and Involves Dynamic Palmitoylation of LAMTOR1 and mTOR. *Frontiers in Cellular Neuroscience*, *13*, 115. https://doi.org/10.3389/fncel.2019.00115

Schmidt, M. F., Bracha, M., & Schlesinger, M. J. (1979). Evidence for covalent attachment of fatty acids to Sindbis virus glycoproteins. *Proceedings of the National Academy of Sciences*, *76*(4), 1687–1691. https://doi.org/10.1073/pnas.76.4.1687

Scinto, S. L., Bilodeau, D. A., Hincapie, R., Lee, W., Nguyen, S. S., Xu, M., Ende, C. W. am, Finn, M. G., Lang, K., Lin, Q., Pezacki, J. P., Prescher, J. A., Robillard, M. S., & Fox, J. M. (2021). Bioorthogonal chemistry. *Nature Reviews Methods Primers*, *1*(1), 30. https://doi.org/10.1038/s43586-021-00028-z

Shahinian, S., & Silvius, J. R. (1995). Doubly-lipid-modified protein sequence motifs exhibit long-lived anchorage to lipid bilayer membranes. *Biochemistry*, *34*(11), 3813–3822. https://doi.org/10.1021/bi00011a039

Stevenson, F. T., Bursten, S. L., Locksley, R. M., & Lovett, D. H. (1992). Myristyl acylation of the tumor necrosis factor alpha precursor on specific lysine residues. *The Journal of Experimental Medicine*, *176*(4), 1053–1062. https://doi.org/10.1084/jem.176.4.1053

Taji, F., Kouchesfahani, H. M., Sheikholeslami, F., Romani, B., Baesi, K., Vahabpour, R., Edalati, M., Teimoori-Toolabi, L., Jazaeri, E. O., & Abdoli, A. (2017). Autophagy induction reduces telomerase activity in HeLa cells. *Mechanisms of Ageing and Development*, *163*, 40–45. https://doi.org/10.1016/j.mad.2016.12.011

Tanida, I. (2011). Autophagosome Formation and Molecular Mechanism of Autophagy. *Antioxidants & Redox Signaling*, *14*(11), 2201–2214. https://doi.org/10.1089/ars.2010.3482

Topinka, J. R., & Bredt, D. S. (1998). N-Terminal Palmitoylation of PSD-95 Regulates Association with Cell Membranes and Interaction with K+ Channel Kv1.4. *Neuron*, *20*(1), 125–134. https://doi.org/10.1016/s0896-6273(00)80440-7

Vesa, J., Su, H., Watts, G. D., Krause, S., Walter, M. C., Martin, B., Smith, C., Wallace, D. C., & Kimonis, V. E. (2009). Valosin containing protein associated inclusion body myopathy: abnormal vacuolization, autophagy and cell fusion in myoblasts. *Neuromuscular Disorders*, *11*. https://doi.org/10.1016/j.nmd.2009.08.003

Wang, H., Sun, H.-Q., Zhu, X., Zhang, L., Albanesi, J., Levine, B., & Yin, H. (2015). GABARAPs regulate PI4P-dependent autophagosome:lysosome fusion. *Proceedings of the National Academy of Sciences*, *112*(22), 7015–7020. https://doi.org/10.1073/pnas.1507263112

Wang, X., Herr, R. A., & Hansen, T. H. (2012). Ubiquitination of Substrates by Esterification. *Traffic*, *13*(1), 19–24. https://doi.org/10.1111/j.1600-0854.2011.01269.x

Wang, Y., Ballar, P., Zhong, Y., Zhang, X., Liu, C., Zhang, Y.-J., Monteiro, M. J., Li, J., & Fang, S. (2011). SVIP Induces Localization of p97/VCP to the Plasma and Lysosomal Membranes and Regulates Autophagy. *PLoS ONE*, *6*(8), e24478. https://doi.org/10.1371/journal.pone.0024478

Witt, C. C., Witt, S. H., Lerche, S., Labeit, D., Back, W., & Labeit, S. (2008). Cooperative control of striated muscle mass and metabolism by MuRF1 and MuRF2. *The EMBO Journal*, *27*(2), 350–360. https://doi.org/10.1038/sj.emboj.7601952

Won, S. J., Kit, M. C. S., & Martin, B. R. (2017). Protein depalmitoylases. *Critical Reviews in Biochemistry and Molecular Biology*, *53*(1), 1–16. https://doi.org/10.1080/10409238.2017.1409191

Wu, J., Wu, J., Yang, L., Wei, L., & Zou, D. (2013). Rosiglitazone protects against palmitate-induced pancreatic beta-cell death by activation of autophagy via 5′-AMP-activated protein kinase modulation. *Endocrine*, *44*(1), 87–98. https://doi.org/10.1007/s12020-012-9826-5

Xia, D., Tang, W. K., & Ye, Y. (2016). Structure and function of the AAA+ ATPase p97/Cdc48p. *Gene*, *583*(1), 64–77. https://doi.org/10.1016/j.gene.2016.02.042

Yamanaka, K., Sasagawa, Y., & Ogura, T. (2012). Recent advances in p97/VCP/Cdc48 cellular functions. *Biochimica et Biophysica Acta (BBA) - Molecular Cell Research*, *1823*(1), 130–137. https://doi.org/10.1016/j.bbamcr.2011.07.001

Yang, M., Jalloh, A. S., Wei, W., Zhao, J., Wu, P., & Chen, P. R. (2014). Biocompatible click chemistry enabled compartment-specific pH measurement inside E. coli. *Nature Communications*, *5*(1), 4981. https://doi.org/10.1038/ncomms5981

Yap, M. C., Kostiuk, M. A., Martin, D. D. O., Perinpanayagam, M. A., Hak, P. G., Siddam, A., Majjigapu, J. R., Rajaiah, G., Keller, B. O., Prescher, J. A., Wu, P., Bertozzi, C. R., Falck, J. R., & Berthiaume, L. G. (2010). Rapid and selective detection of fatty acylated proteins using ω-alkynyl-fatty acids and click chemistry. *Journal of Lipid Research*, *51*(6), 1566–1580. https://doi.org/10.1194/jlr.d002790

Yeo, B. K., & Yu, S.-W. (2016). Valosin-containing protein (VCP): structure, functions, and implications in neurodegenerative diseases. *Animal Cells and Systems*, *20*(6), 303–309. https://doi.org/10.1080/19768354.2016.1259181

Yin, J., Wang, Y., Gu, L., Fan, N., Ma, Y., & Peng, Y. (2015). Palmitate induces endoplasmic reticulum stress and autophagy in mature adipocytes: Implications for apoptosis and inflammation. *International Journal of Molecular Medicine*, *35*(4), 932–940. https://doi.org/10.3892/ijmm.2015.2085

Zaballa, M.-E., & van der Goot, F. G. (2018). The molecular era of protein S-acylation: spotlight on structure, mechanisms, and dynamics. *Critical Reviews in Biochemistry and Molecular Biology*, *53*(4), 1–31. https://doi.org/10.1080/10409238.2018.1488804

Zaręba-Kozioł, M., Figiel, I., Bartkowiak-Kaczmarek, A., & Włodarczyk, J. (2018). Insights Into Protein S-Palmitoylation in Synaptic Plasticity and Neurological Disorders: Potential and Limitations of Methods for Detection and Analysis. *Frontiers in Molecular Neuroscience*, *11*, 175. https://doi.org/10.3389/fnmol.2018.00175

Zhou, F., Xue, Y., Yao, X., & Xu, Y. (2006). CSS-Palm: palmitoylation site prediction with a clustering and scoring strategy (CSS). *Bioinformatics*, *22*(7), 894–896. https://doi.org/10.1093/bioinformatics/btl013